Clim. Past, 18, 1915–1945, 2022
https://doi.org/10.5194/cp-18-1915-2022

Climate of the Past
Open Access
EGU

A 300 000-year record of cold-water coral mound build-up at the East Melilla Coral Province (SE Alboran Sea, western Mediterranean)

Robin Fentimen[1,a], Eline Feenstra[1], Andres Rüggeberg[1], Efraim Hall[1], Valentin Rime[1], Torsten Vennemann[2], Irka Hajdas[3], Antonietta Rosso[4], David Van Rooij[5], Thierry Adatte[2], Hendrik Vogel[6], Norbert Frank[7], and Anneleen Foubert[1]

[1]Department of Geosciences, University of Fribourg, Fribourg, 1700, Switzerland
[2]Institute of Earth Surface Dynamics, University of Lausanne, Lausanne, 1015, Switzerland
[3]Laboratory of Ion Beam Physics, ETH Zürich, Zürich, 8093, Switzerland
[4]Department of Biological, Geological and Environmental Sciences, University of Catania, Catania, 95128, Italy
[5]Department of Geology, Ghent University, Ghent, 9000, Belgium
[6]Institute of Geological Sciences and Oeschger Centre for Climate Change Research, University of Bern, Bern, 3012, Switzerland
[7]Institute of Environmental Physics, University of Heidelberg, 69120 Heidelberg, Germany
[a]present address: Réserves Naturelles de France – Antenne Littorale, Terre Plein de l'Ecluse, 50400, Granville, France

Correspondence: Robin Fentimen (robin.fentimen@ens-lyon.fr)

Received: 18 November 2021 – Discussion started: 14 January 2022
Revised: 28 June 2022 – Accepted: 23 July 2022 – Published: 24 August 2022

Abstract. This study provides a detailed reconstruction of cold-water coral mound build-up within the East Melilla Coral Province (southeastern Alboran Sea), more precisely at the northern part of Brittlestar Ridge I, over the last 300 kyr. The multiproxy investigation of core MD13-3462G reveals that mound build-up took place during both interglacial and glacial periods at average aggradation rates ranging between 1 and 10 cm kyr^{-1}. These observations imply that corals never thrived but rather developed under stressful environmental conditions. Maximum aggradation rates of 18 cm kyr^{-1} are recorded during the last glacial period, hence providing the first evidence of coral mound development during this time period in the western Mediterranean. The planktonic (*Globigerina bulloides*) and benthic (*Lobatula lobatula*) δ^{18}O records from core MD13-3462G show typical interglacial–glacial variations during the last two interglacial–glacial cycles. This is in contrast with δ^{18}O records generally recovered from coral mounds and highlights that the northern part of Brittlestar Ridge I experienced reduced albeit relatively continuous accretion. High abundances of infaunal benthic foraminifera (*Bulimina marginata*, *Bulimina striata*, and *Uvigerina mediterranea*) suggest that weak seafloor oxygenation associated with important terrestrial organic matter input characterized interglacial periods, whilst the dominance of large epibenthic species (*Discanomalina coronata* and *Lobatula lobatula*) and Miliolids is probably linked to stronger Levantine Intermediate Water circulation and fresher organic matter input during glacial periods. In addition, the computed tomography (CT) quantification of macrofaunal remains shows that the bryozoan *Buskea dichotoma* is present throughout the entire 300 kyr of mound build-up history, with the exception of MIS 5, and is possibly a key contributor to mound development during glacial periods. The comparison of our observations to other long-term coral mound records demonstrates that western and central Mediterranean coral mounds do not show concurrent build-up over interglacial–glacial cycles, implying that their development may be driven by regional and local environmental forcing.

1 Introduction

Cold-water coral (CWC) reefs are diverse marine ecosystems that are widespread in the world's oceans (Freiwald et al., 2004; Roberts et al., 2009). The most important reef-building CWC species in the Atlantic Ocean and Mediterranean Sea are the scleractinian species *Desmophyllum pertusum* (formerly known as *Lophelia pertusa*, see Addamo et al., 2016) and *Madrepora oculata* (Roberts et al., 2009). These predominantly suspension-feeding organisms depend on enhanced hydrodynamic regimes that provide food to their polyps (White et al., 2005; Mienis et al., 2007; Carlier et al., 2009; Davies et al., 2009; Roberts et al., 2009; Hanz et al., 2019). The role played by internal waves (i.e. waves that occur at the interface between two water masses of different densities) in the proliferation of CWCs is vital, since these oscillations increase turbulence, and hence nutrient supply, and accumulate particulate organic matter due to their sharp density gradient (White et al., 2005; Davies et al., 2009; Pomar et al., 2012; Wang et al., 2019). Physico-chemical properties of the ambient water (e.g. salinity, temperature, dissolved oxygen concentrations, pH, density) also affect CWC growth (Freiwald et al., 2004; Dullo et al., 2008; Davies and Guinotte, 2011; Hanz et al., 2019). If favourable conditions are maintained over longer periods, successive reef generations may build CWC mounds through the interaction between coral growth and sediment accumulation (Wilson, 1979; Roberts et al., 2006; Foubert and Henriet, 2009; Roberts et al., 2009; Hebbeln et al., 2016). Consequently, CWC mounds can reach considerable heights of over 300 m and spread for kilometres in width and length at their base (De Mol et al., 2002; Kenyon et al., 2003; Huvenne et al., 2005). Mound development may span from thousands to millions of years and attain important mound aggradation rates, e.g. $\pm 400\,\mathrm{cm\,kyr^{-1}}$ in the East Melilla Coral Province (EMCP; Frank et al., 2009; López Correa et al., 2012; Fink et al., 2013; Stalder et al., 2015; Wienberg et al., 2018). As such, and in spite of mound formation being generally discontinuous, CWC mounds are valuable environmental and climate archives (Rüggeberg et al., 2007; Roberts et al., 2009). Moreover, the sensitivity of CWCs to climate change is useful to monitor variations in environmental conditions (e.g. water mass variability, surface productivity, bottom current velocity; Rüggeberg et al., 2007; Huvenne et al., 2009; Hebbeln et al., 2016; Wienberg et al., 2018, 2020).

The long-term development of CWC mounds was first studied in the NE Atlantic Ocean, where it was shown to follow large-scale changes in oceanographic conditions (e.g. De Mol et al., 2002; Dorschel et al., 2005; Frank et al., 2011; Wienberg et al., 2018, 2020). Coral mounds along the Irish margin form during interglacial and interstadial times, whilst they decline during glacial periods (Dorschel et al., 2005; Kano et al., 2007; Rüggeberg et al., 2007; Eisele et al., 2008). The same distribution pattern has been observed for CWC mounds situated in the NW Atlantic Ocean (Matos et al., 2015; 2017). In these two regions, CWC development is tightly knitted to the formation of internal waves and increased turbulence at the limit between water masses (White, 2007; Mohn et al., 2014; Raddatz et al., 2014; Matos et al., 2015, 2017; Hebbeln et al., 2016; Wienberg et al., 2020). At lower latitudes in the eastern Atlantic, off the coast of Mauritania and in the Gulf of Cádiz, coral mounds form essentially during glacial times (Wienberg et al., 2009; Eisele et al., 2011).

In the Mediterranean Sea, CWC mound provinces are concentrated in the Alboran Sea (Fink et al., 2013, 2015; Lo Iacono et al., 2014; Stalder et al., 2015, 2018; Terhzaz et al., 2018; Hebbeln, 2019; Wang et al., 2019; Fentimen et al., 2020a; Rachid et al., 2020; Corbera et al., 2021; Sánchez-Guillamón et al., 2022), the Corsica Channel (Remia and Taviani, 2005; Angeletti et al., 2020), the Strait of Sicily (Martorelli et al., 2011), the northern Ionian Sea (Carlier et al., 2009; Freiwald et al., 2009), and on the Tunisian Plateau (Camafort et al., 2020; Corbera et al., 2022). Except for the North Cabliers Coral Mound Province situated in the central part of the eastern Alboran Sea (Fig. 1b), the northern Ionian Sea mounds (i.e. Santa Maria di Leuca CWC mounds), and the Corsica Channel mounds, the above-mentioned CWC mounds are all at present in a stagnation phase with little or no corals living at their surfaces (Corbera et al., 2019; Hebbeln, 2019; Angeletti et al., 2020; Sánchez-Guillamón et al., 2022).

The Melilla Mound Field is the largest CWC province in the Alboran Sea, covering an area greater than $500\,\mathrm{km^2}$ parallel to the margin (Comas and Pinheiro, 2010; Lo Iacono et al., 2014). It can be divided into two provinces, the West and East Melilla Coral Provinces (EMCP), respectively situated 7 km northwest and 35 km northeast of the Cape Tres Forcas (Lo Iacono et al., 2014; Fig. 1b). Within the EMCP, the localities of Brittlestar Ridge I (BRI) and Dragon Mound have received the most attention during the last decade (Fig. 1b and c; Fink et al., 2013, 2015; Stalder et al., 2015, 2018; Terhzaz et al., 2018; Hebbeln, 2019; Fentimen et al., 2020a; Krengel, 2020; Rachid et al., 2020; Wang et al., 2021). U-series dating of corals revealed that the formation of Dragon Mound began 450 kyr ago, whereas BRI started building up over 538 kyr ago (Krengel, 2020). Mound development at Dragon Mound essentially took place during the last interglacial periods (MIS 9, 7, and 5) at rates varying between 26 and $83\,\mathrm{cm\,kyr^{-1}}$, although a number of glacial coral occurrences were recorded during MIS 10 and MIS 8 (Krengel, 2020). Krengel (2020) also observed interglacial mound build-up phases at BRI, more precisely during MIS 9 and MIS 7 at rates between 17 and $25\,\mathrm{cm\,kyr^{-1}}$. Similar to Dragon Mound, glacial periods at BRI appear to host sporadic phases of coral development, noticeably during MIS 12 and MIS 4 (Krengel, 2020). In contrast to Dragon Mound, the early Holocene and Bølling–Allerød interstadial marked a rapid phase of mound aggradation at BRI (75–$420\,\mathrm{cm\,kyr^{-1}}$; Fink et al., 2013; Stalder et al., 2015, 2018;

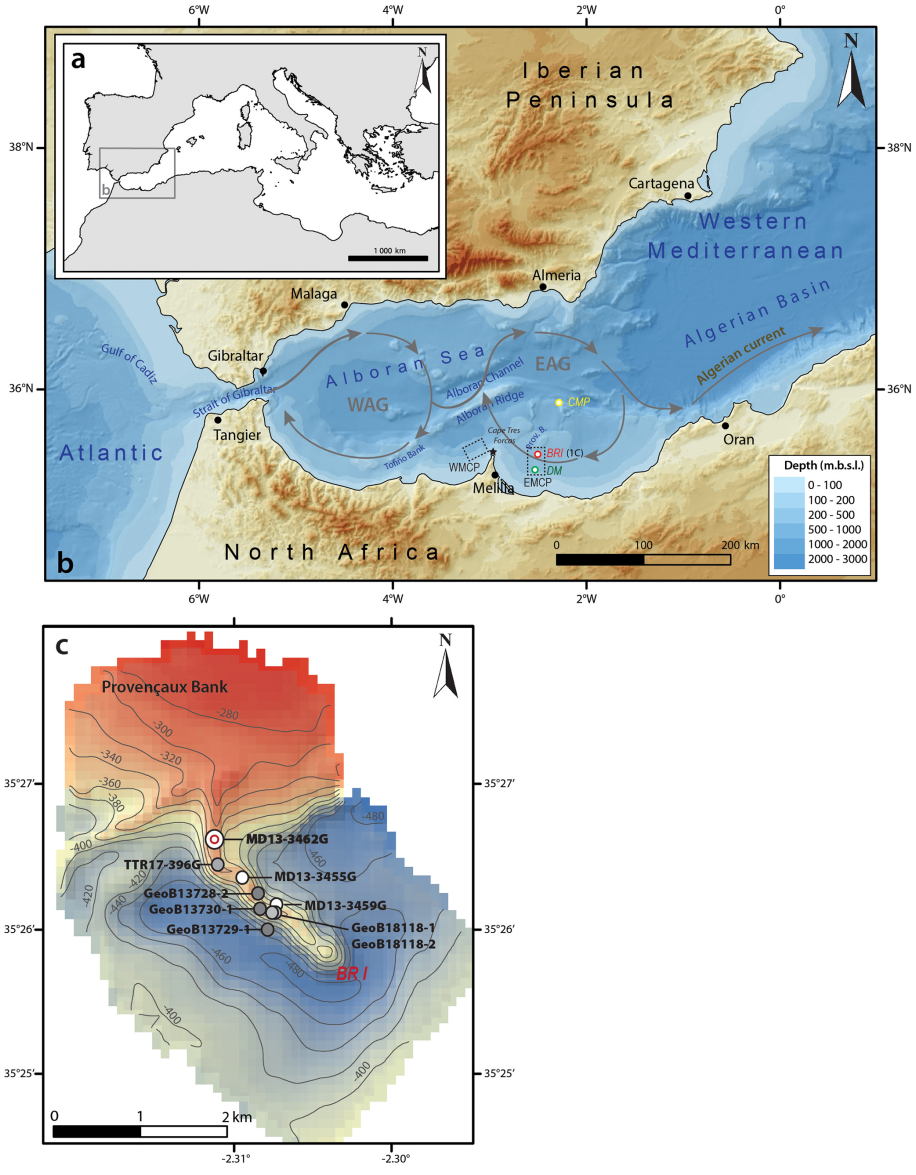

Figure 1. Location of the study area. **(a)** General map of the Mediterranean Sea and location of the investigated region. **(b)** Bathymetric map of the western Mediterranean Sea based on the GEBCO_2019 gridded bathymetric data. Yellow, red, and green dots respectively indicate the locations of the Cabliers Coral Mound Province (CMP), Brittlestar Ridge I (BRI), and Dragon Mound (DM). Additional abbreviations: EMCP – East Melilla Coral Province; WMCP – West Melilla Coral Province; WAG – Western Alboran Gyre; EAG – Eastern Alboran Gyre. **(c)** Bathymetry and location of the Provençaux Bank and Brittlestar Ridge I (BRI). The location of the studied core MD13-3462G recovered during cruise GATEWAY no. 194 on board the research vessel *Marion Dufresne II* (Van Rooij et al., 2017) is indicated together with other cores previously acquired and investigated in the area (GeoB13728-2, GeoB13730-1, and GeoB13729-1: Fink et al., 2013; TTR17-396G: Stalder et al., 2018; MD13-3455G: Fentimen et al., 2020; GeoB18118-1 and GeoB18118-2: Krengel, 2020).

Fentimen et al., 2020a; Krengel, 2020) and at mounds situated in the West Melilla Coral Province (12–176 cm kyr^{-1}; Wang et al., 2019).

The predominant occurrence of CWCs during interglacial periods noticed by Krengel (2020) in the EMCP is also observed during the last four interglacial–glacial cycles in the South Cabliers Mound Province, although mound build-up in the latter is the most important during deglacials and temperate interstadials (Corbera et al., 2021). In contrast, over the last 400 kyr, the Tunisian Coral Mound Province situated in the central Mediterranean experienced its most marked phase of coral development during the last glacial period, whereas interglacial periods were particularly scarce in coral occurrences (Corbera et al., 2022). These different temporal distributions suggest that mound build-up in the western and central Mediterranean Sea does not follow a uniform

pattern. Although the development of coral communities at the EMCP during the last 30 kyr is well-documented and novel long-term records are emerging from the western and central Mediterranean Sea (Krengel, 2020; Corbera et al., 2021, 2022), the long-term environmental forcing affecting the EMCP still remains little documented. The aims of this study are hence (1) to constrain the environmental parameters driving CWC mound formation in the EMCP over the last 300 kyr and (2) to assess the heterogeneities in long-term CWC mound formation within the western Mediterranean Sea.

2 Study area

2.1 Geological setting

The Alboran Sea is the westernmost basin of the Mediterranean Sea and is closely connected to the Atlantic Ocean by the Strait of Gibraltar. It is approximately 400 km long, with a width of 200 km, an average depth of 1300 m, and a maximum depth of 1800 m (Olivet et al., 1973; Comas et al., 1999). The Alboran Sea's metamorphic basement is intruded by a number of volcanic plateaus and seamounts formed through the extensional processes that took place between 17 and 8 million years ago (Comas et al., 1999; Duggen et al., 2008). One of these shallow volcanic plateaus, the Provençaux Bank (ca. 200 m depth), extends in a series of three ridges colonized by CWCs named the "Brittlestar ridges" (BRI, BRII, BRIII) (Comas et al., 2009; Fink et al., 2013). They are part of the larger EMCP nestled at depths between 250 and 450 m. The ridges are 3 to 20 km in length and vary in height from 50 to 150 m (Hebbeln, 2019). These mounds are characterized by dead coral framework with some living corals at their summits and erosional moats at their base, supporting the presence of dynamic currents in the area (Hebbeln, 2019) (Fig. 1c).

2.2 Oceanography

Low-salinity (ca. 36.5 PSU), low-density Atlantic Water enters the Mediterranean through the Strait of Gibraltar. This inflowing water mass mixes with Mediterranean water while crossing the Strait of Gibraltar to form the Modified Atlantic Water (MAW), the dominant surface water mass in the Alboran Sea (La Violette, 1983; Millot, 2009). In addition, evaporation also exceeds river runoff and precipitation; hence, MAW becomes saltier and denser journeying east and finally sinks in the Levantine, Aegean, Adriatic, and Liguro–Provençal sub-basins (Millot et al., 2006). Intermediate waters consist of the highly saline (ca. 38.5 PSU) and warm (ca. 13.5 °C) Levantine Intermediate Water (LIW) that forms in the Levantine basin and flows from east to west, entering the western Mediterranean through the Strait of Sicily to finally exit through the Strait of Gibraltar (Millot, 2013). Levantine Intermediate Water contributes to ca. 70 % of the total outflow of Mediterranean Outflow Water (MOW; Millot, 2013) and flows between 200 and 600 m water depth in the Alboran Sea, whilst the core of the LIW is situated at approximately 400 m depth (Millot, 2009).

It is important to note that, as it moves towards the west, the LIW receives contributions from other water masses, and hence its characteristics gradually change as it gets closer to the Strait of Gibraltar (Millot, 2013). Moreover, intermediate waters appear to differ between the northern and southern Alboran Sea (Fig. 2). Brittlestar Ridge I lays in the depth range of LIW (Fig. 2). Western Mediterranean Deep Water makes up the deepest water mass, flowing under the LIW (Millot and Taupier-Letage, 2005). It forms in the Gulf of Lion and flows westward to finally exit through the Strait of Gibraltar and contributes to the deeper MOW (Millot et al., 2006). In the Alboran Sea, WMDW principally circulates along the Moroccan margin (Millot and Taupier-Letage, 2005).

The surface MAW extends down to approximately 200 m depth (Katz, 1972) and enters the northwestern Alboran Sea as a jet (1.6 Sv; $1\,\mathrm{Sv} = 10^6\,\mathrm{m}^3\,\mathrm{s}^{-1}$; Lanoix, 1974). This jet triggers the formation of the quasi-permanent anti-cyclonic Western Alboran Gyre that contributes to mixing between surface MAW and underlying LIW (Heburn and La Violette, 1990; Lafuente et al., 1998). When the waters of the Western Alboran Gyre reach the African coast, they separate into two branches: one flows back westward along the coast towards the Strait of Gibraltar, while the other flows towards the eastern part of the basin to form the Eastern Alboran Gyre (La Violette, 1983; Viúdez and Tintoré, 1995). This second non-permanent gyre also contributes to the mixing process between surface and intermediate water masses. The Provençaux Bank and Brittlestar Ridge I are situated in the path of the westward-circulating branch of the Eastern Alboran Gyre (Lanoix, 1974; Viúdez and Tintoré, 1995; Fig. 1). The mixing between surface and intermediate water masses occurs down to ca. 30 m water depth (Heburn and La Violette, 1990). The Strait of Gibraltar is a shallow (ca. 300 m depth) and narrow (ca. 20 km wide) crossing point for entering lower-salinity MAW and exiting higher-salinity MOW (Heburn and La Violette, 1990; Millot, 2009). Thus, the Strait of Gibraltar plays a key role in controlling water mass exchanges between the semi-enclosed Mediterranean Sea and the Atlantic Ocean. The importance of the water exchange varies between glacial and interglacial periods as a function of sea level change. Moreover, the narrow width and depth of the Strait of Gibraltar, together with the geometry of the Alboran basin and the Coriolis force, affects the formation, mean position, and shape of the Alboran gyres (Heburn and La Violette, 1990). Thus, this will in turn affect mixing between surface and intermediate water masses in the Alboran Sea.

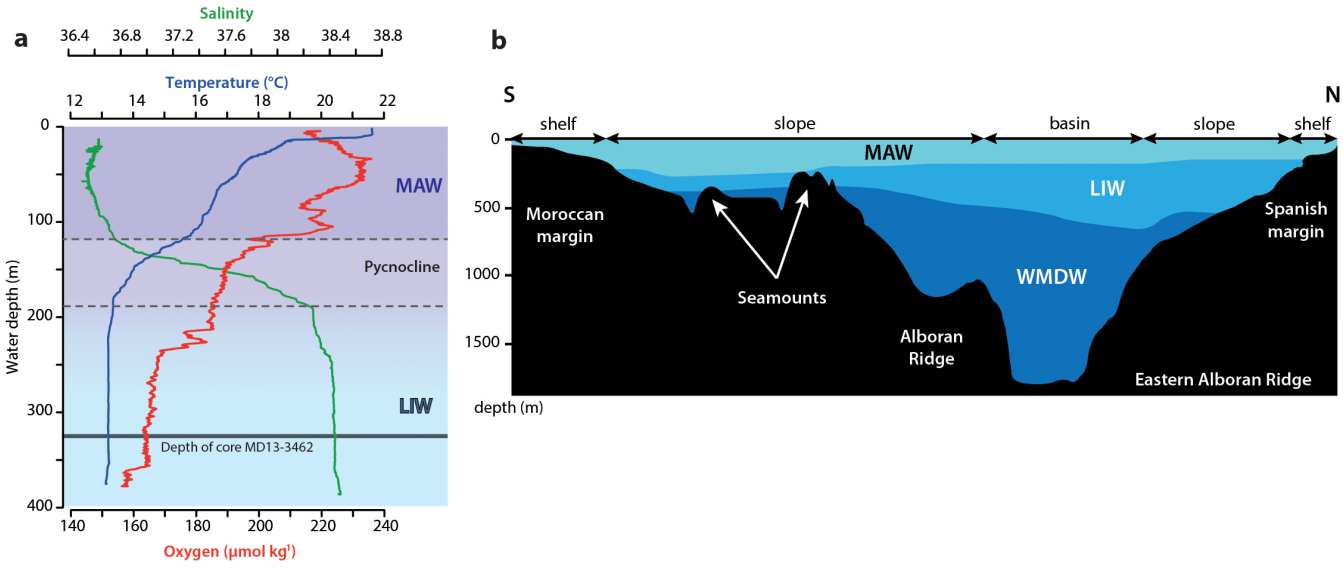

Figure 2. **(a)** CTD profile taken at the east of Brittlestar Ridge I (35°26.087′ N; 2°30.100′ W) during the cruise GATEWAY (no. 194) on board the research vessel *Marion Dufresne II* in June 2013 (Van Rooij et al., 2017). Salinity (PSU), temperature (°C), and oxygen content (µmol kg^{-1}) are indicated. The location of core MD13-3462G in relation to the profile is indicated by the black line. **(b)** North–south-orientated bottom-water profile of the eastern Alboran Sea modified from Ercilla et al. (2016). Abbreviations: MAW – Modified Atlantic Water, LIW – Levantine Intermediate Water, WMDW – Western Mediterranean Dense Water.

3 Material and methods

3.1 Sample collection

This study is based on the multiproxy analysis of gravity core MD13-3462G (35°26.531′ N, 2°31.073′ W; 327 m depth; 926 cm long) recovered during the EUROFLEETS cruise MD194 Gateway on board the R/V *Marion-Dufresne II* (Van Rooij et al., 2017). Cores were split frozen and sedimentary facies descriptions were made at the University of Fribourg prior to sampling. These descriptions include a detailed investigation of the texture, grain size, and colour of the matrix sediment, together with the identification and assessment of the preservation state of major macrofaunal components (Fig. 3). All data were plotted using the ggplot2 package for R (Wickham, 2016; R Core Team, 2018).

3.2 Macrofaunal quantification

X-ray computed tomography (CT) imaging was carried out on whole-round sections using a Siemens Somatom Definition AS64 at the Institute of Forensic Sciences at the University of Bern (Switzerland). Core sections were scanned using an X-ray source operating at 120 kV. The images were reconstructed with a slice thickness of 0.6 mm taking into account an increment of 0.3 mm, whilst the pixel resolution of the slices is 0.3 mm. The Avizo 9.4 software was used to visualize, segment, and quantify the volumes of the main macrofaunal components (coral, bryozoan, and bivalve–brachiopod fragments). Prior to segmentation, images were filtered to remove noise in the matrix using a non-local means filter. Brachiopods and bivalves were segmented manually. Corals, matrix, pores, and bryozoans were segmented through the combination of dual thresholding and watershed segmentation. Labelled fragments smaller than 5 voxels were filtered prior to quantification. The MaterialStatistics module was used to quantify the vol % of faunal fragments per slice, and the same volume of interest was selected for each core section.

3.3 Geochemical logging

Geochemical logging was performed using the Itrax high-resolution X-ray fluorescence (XRF) core scanner on split cores at the Institute of Geological Sciences, University of Bern (Switzerland). Measurements were taken at 5 mm intervals using an integration time of 20 s at 30 kV and 45 mA. To counter potentially biased measurements linked to the uneven surface of CWC cores, such as the direct measurement of air or of CWC skeletons, a three-step post-treatment of the dataset was carried out. First, X-ray fluorescence values with argon counts higher than 6000, representing the measurement of air and thereby more porous and/or cracked media not representative of changes in matrix sediment composition, were removed from the final dataset. Secondly, each individual measurement point was compared to high-resolution core images to assess if the measurement was taken on the matrix sediment or not. Finally, elemental counts were normalized by a conservative (minor) element of the background sediment (i.e. aluminium). Aluminium can be used effectively to counter variations in coral content (Löwemark et al., 2011). Normalization of the minor elements with Al is effec-

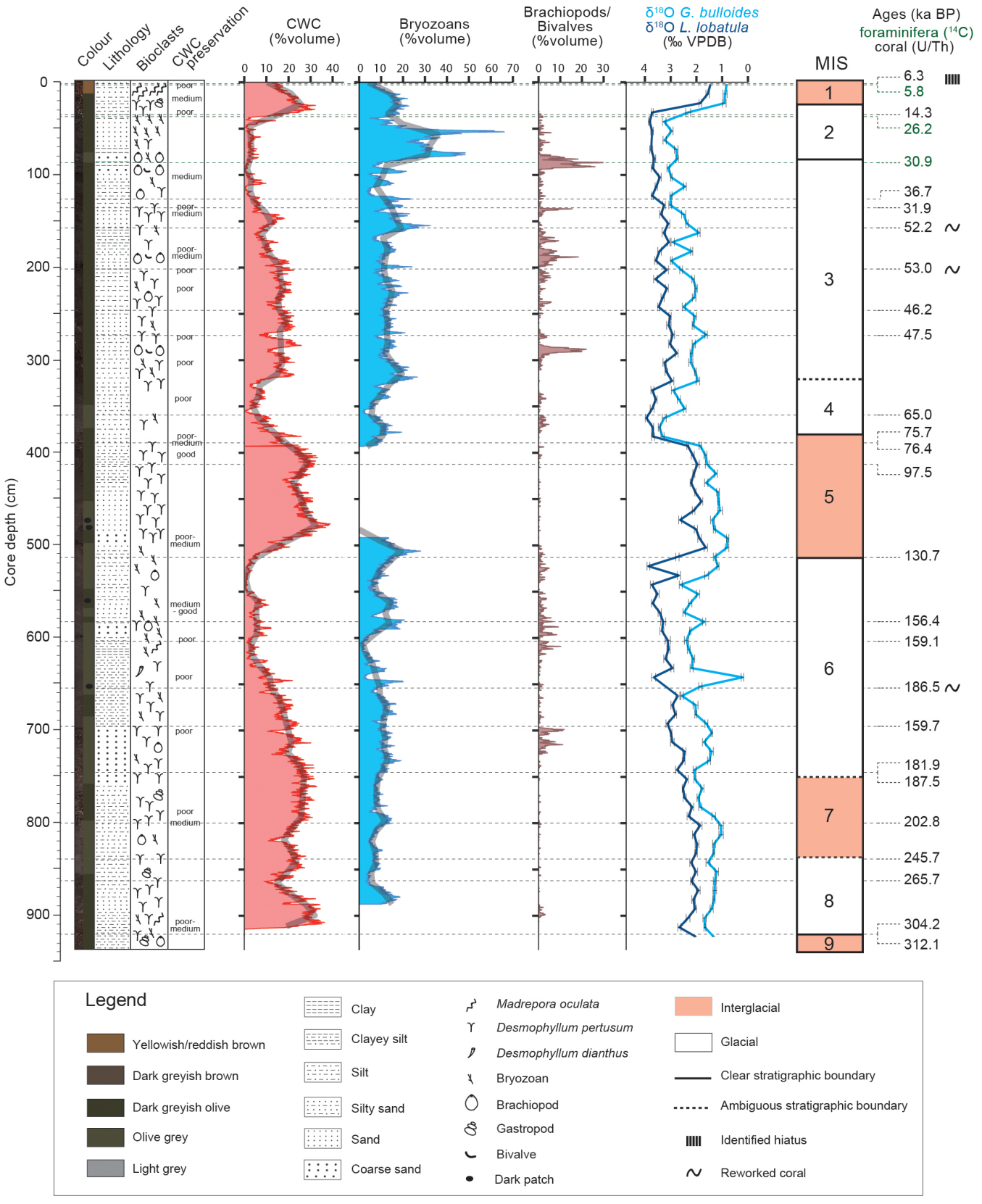

Figure 3. Core description, stratigraphy, and macrofaunal composition of core MD13-3462G. Stratigraphy is based on the planktonic (*G. bulloides*) and benthic (*L. lobatula*) δ^{18}O records (‰ VPDB), the uranium-series ages of coral fragments, and the epibenthic foraminiferal radiocarbon ages for the first metre of the core (see Fig. 4).

tive when the detrital–terrestrial contribution to the sediment is high. Indeed, aluminium generally behaves conservatively and can hence be used to assess the relative variations of specific elements in sedimentary records (Calvert and Pedersen, 2007, and references therein; Löwemark et al., 2011; Rodrigo-Gámiz et al., 2011; Martinez-Ruiz et al., 2015)

In this study, we use the $\log_{10}$ normalized (Gregory et al., 2019) Si/Al ratio as a proxy for terrestrial (fluvial and aeolian) input. Indeed, the Saharan region is the dominant source of aeolian dust in the Mediterranean Sea and is essentially composed of silicates with high quartz content (Guieu and Thomas, 1996; Caquineau et al., 1998, 2002). Moreover, these are rare in Alboran Sea sediments (Masqué et al., 2003), hence the applicability of Si/Al ratio to track variations in terrestrial input. In combination with information provided by benthic foraminiferal assemblages, the $\log_{10}$ normalized the Si/Al ratio provides a robust and valuable record of terrestrial input.

3.4 Grain size analysis and organic geochemistry

The grain size of the siliciclastic fraction was analysed using the Malvern Mastersizer 3000 at the Department of Geology, Ghent University (Belgium). The core was sampled with a small spoon (1 cm^3) every 5 cm. Large clasts (> 1 cm), such as coral or bryozoan fragments, were sieved out prior to analysis. Samples were placed in 35 % H_2O_2 to remove organic matter and boiled until the reaction ended. Following this first step, samples were boiled in 10 % HCl for 2 min to dissolve $CaCO_3$. Prior to measurement, samples were placed in 2 % sodium polymetaphosphate and boiled to assure complete disaggregation. Any remaining particle larger than 2 mm was sieved out before measurement. A total of 87 size classes were measured (from 0.01 to 2000 µm). Each sample was measured three times and results were then averaged. The mean grain size of the siliciclastic fraction $\overline{GS}$ (Folk and Ward, 1957) was calculated for the entire dataset with the Rysgran package for R (Gilbert et al., 2015; R Core Team, 2018). The sortable silt mean size $\overline{SS}$, as defined by McCave et al. (1995, i.e. the mean of the 10–63 µm grain size range), was also calculated following the same procedure. Furthermore, following McCave and Hall (2006), the percentage of sortable silt (SS %) in the total <63 µm fraction was calculated. This percentage, together with the sortable silt mean size, was used as an indication of bottom current velocity (McCave and Hall, 2006; Toucanne et al., 2012). It has to be mentioned that the use of $\overline{SS}$ as a proxy for bottom current velocity on cores recovered from CWC mounds may be biased (e.g. Eisele et al., 2011). Indeed, the baffling effect of the coral framework can locally reduce bottom current velocity and favour the deposition of fine sediments (Huvenne et al., 2009; Titschack et al., 2009; Fentimen et al., 2020b), thus leading to an underestimation of $\overline{SS}$ during periods with high CWC content. Because of this, only relative increases in $\overline{SS}$ are considered in combination with results obtained from other proxies.

Total organic carbon (TOC, wt %) and mineral carbon (MinC, wt %) contents were determined on matrix sediments every 10 cm using the Rock-Eval6 technique at the Laboratory of Sediment Geochemistry at the University of Lausanne (Fantasia et al., 2019). The Rock-Eval6 technique produces an oxygen and hydrogen index, respectively corresponding to the quantity of CO_2 relative to TOC and the quantity of pyrolyzable organic compounds relative to TOC (Fantasia et al., 2019). These two indices give an indication of the origin of the organic matter present in the samples (Van Krevelen, 1993).

3.5 Microfaunal and macrofaunal investigations

The core was sampled (sliced) every 10 cm for micropaleontological analysis. Samples were weighed dry, washed through a 63 µm mesh sieve, and dried at 30 °C. Each fraction was then dry-sieved through a series of 63, 125, and 2000 µm mesh sieves and weighed. A target number of 300 benthic foraminifera were identified from the fraction larger than 125 µm for each sample. If the residue contained more than 600 specimens, it was split using a dry microsplitter. Relative abundances (%) of benthic species were calculated from the total benthic foraminiferal assemblage. The benthic foraminiferal density was calculated by dividing the total number of foraminifera of a given sample by the sample fraction's weight. The diversity Shannon index (H') was computed using the PRIMER6 software (Clarke and Gorley, 2006).

Samples prepared for micropaleontological analysis were further used to identify bryozoan species and genera at the Department of Biological, Geological and Environmental Sciences, University of Catania (Italy), on the 12 µm to 2 mm and > 2 mm sized fractions. Key intervals with high bryozoan content, previously identified by CT imagery, were selected. Dominant scleractinian corals and main brachiopod and bivalve species were identified at the lowest taxonomic level possible on the > 2 mm sized fraction at the Department of Geosciences, University of Fribourg (Switzerland).

3.6 Radiometric dating

Radiocarbon dating was performed on benthic foraminifera from three samples from the upper first metre of core MD13-3462G at the Laboratory of Ion Beam Physics, ETH Zürich, Switzerland (Table 1). The epibenthic foraminifera species *Discanomalina coronata*, *Lobatula lobatula*, and *Cibicides refulgens* were picked in order to obtain between 4 and 10 mg of pure carbonate. The samples were first dissolved in phosphoric acid. The resulting extracted CO_2 was then converted to graphite and measured by the accelerator mass spectrometry (AMS) technique using the MICADAS dedicated instrument (Synal et al., 2007). Results were corrected for ^{13}C and

calibrated using the Marine13 calibration curve (Reimer et al., 2013) and the software OxCal v4.2.4 (Ramsey, 2017). A reservoir age of 390 ± 80 years was applied to all ages (Siani et al., 2000).

Uranium-series dating was carried out on 24 CWC fragments (*D. pertusum* and *M. oculata*) using a multicollector inductively coupled plasma source mass spectrometer (MC-ICPMS; Thermo Fisher Scientific Neptune^{plus}) coupled with a dissolver (Aridus I) at the Institute of Environmental Physics, Heidelberg University (Table 2). In order to constrain the chronostratigraphy of the core, well-preserved coral fragments were selected at the upper and lower boundaries of coral-rich units. These were identified based on visual core descriptions and CT analysis (macrofaunal quantification; Fig. 3). Coral fragments were physically cleaned with a Dremel® drill tool as well as by sand-blasting and further chemically cleaned using a weak acid leaching prior to measurements. The detailed sample protocol is described by Frank et al. (2004), while spectrometry and chemical U and Th extraction as well as purification followed Wefing et al. (2017). Uranium-series coral ages were used to calculate mound aggradation rates.

3.7 Oxygen and carbon stable isotope analysis

Stable oxygen and carbon isotope compositions were measured on 5 to 12 specimens of the planktonic foraminifera *Globigerina bulloides* and the benthic foraminifera *L. lobatula* from the size fraction 212–250 µm in order to prevent any ontogenic effect on the measurements (Schiebel and Hemleben, 2017). The specimens were first cleaned three times with distilled water in an ultrasonic bath for 2 s. The measurements were then made using a Thermo Fisher Scientific GasBench II connected to a Thermo Finnigan Delta Plus XL isotope ratio mass spectrometer at the Stable Isotope Laboratory of the University of Lausanne (Switzerland) according to the method adapted from Spötl and Vennemann (2003). Results are reported in the conventional δ values in permil (‰) relative to the Vienna Pee Dee Belemnite (VPDB) standard. Analytical standard deviations (1σ) average 0.04 ‰ for δ^{13}C and 0.06 ‰ for δ^{18}O values based on eight replicate analyses of standards in each sequence of 40 samples.

4 Results

4.1 Chronostratigraphy

The chronostratigraphy of core MD13-3462G is based on the combination of the coral ages (U-series dating), the planktonic and benthic stable oxygen isotope records, and the foraminiferal radiocarbon ages for the top first metre of the core (Figs. 3 and 4). The U-series coral ages indicate that core MD13-3462G extends approximately from 300 ka BP (Marine Isotope Stage 9) to the Holocene (Figs. 3 and 4, Table 2). Coral ages have been widely used to define the chronology of cores recovered from coral mounds. This approach provides satisfying results, although age reversals down-core have to be taken into account (e.g. Rüggeberg et al., 2007; Frank et al., 2009; Matos et al., 2017). Indeed, reefs are fragile structures and can collapse, topple, and fragment through the action of bioerosion, strong bottom currents, and gravity-driven processes, resulting in transport and redeposition of coral fragments (Beuck et al., 2005; Dorschel et al., 2007; White, 2007). In contrast, constructing a continuous age model based on stable isotope records is generally considered untrustworthy for cores collected from coral mounds since sedimentation is intermittent (e.g. Dorschel et al., 2005). However, coral ages at the upper and lower boundaries of coral build-up phases in core MD13-3462G (e.g. at 390 and 507 cm depth) correspond to changes in the stable oxygen isotope records (Fig. 3), which in turn match the changes between Marine Isotope Stages (MISs; Lisiecki and Raymo, 2005). As such, the stable oxygen isotope records can, in the case of core MD13-3462G and in conjunction with coral ages, indicate important stratigraphic boundaries (Fig. 4). This is particularly relevant during times when CWCs did not grow and hence cannot serve to construct a timeframe. Stable oxygen isotope records were hence correlated with the reference LR04 stack (Lisiecki and Raymo, 2005) for the δ^{18}O stratigraphy (see Fig. 4a). Tie points were visually identified and a best correlation coefficient determined using Lineage in the software package AnalySeries v. 2.0.8 (Paillard et al., 1996; Table 3). A clear subdivision into glacial–interglacial stages and substages was possible for Marine Isotope Stages (MISs) 1 to 6 with a Pearson's correlation coefficient of $r = 0.79$ ($p < 0.001$), in good agreement with the CWC U-series age dates (see Fig. 4b). However, the correlation became difficult below 650 cm core depth (> 150 ka) due to the resolution of sampling (10 cm), the lower sedimentation rate, and possible hiatuses and reworking units flattening the curve. Therefore, U-series ages were used to correlate the lower part of the core, resulting in a Pearson's correlation coefficient of $r = 0.51$ ($p < 0.009$). The foraminiferal δ^{18}O records still follow the LR04 stack until late MIS 7, but the signal remains at relatively light δ^{18}O values for the bottom ∼ 100 cm of MD13-3462G covering a time span of around 100 kyr (Fig. 4b).

The stratigraphic boundaries from the base of the core to ca. 650 cm depth were defined based on the U-series coral ages, as planktonic stable oxygen isotope compositions show little variation. The boundaries of MIS 8 are the most poorly defined. Due to difficulties precisely defining the stratigraphy of this section of the core, it will not be considered in detail during this study. In contrast, the planktonic and benthic δ^{18}O values and the coral ages do constrain the stratigraphic boundaries from MIS 6 to MIS 1 (Fig. 4). Contrary to sediment records from CWC mounds of the North Atlantic, where no clear glacial or interglacial δ^{18}O values are reported (e.g. Dorschel et al., 2005; Rüggeberg et al., 2007; Eisele et al., 2008; Mienis et al., 2009), core MD13-3462G

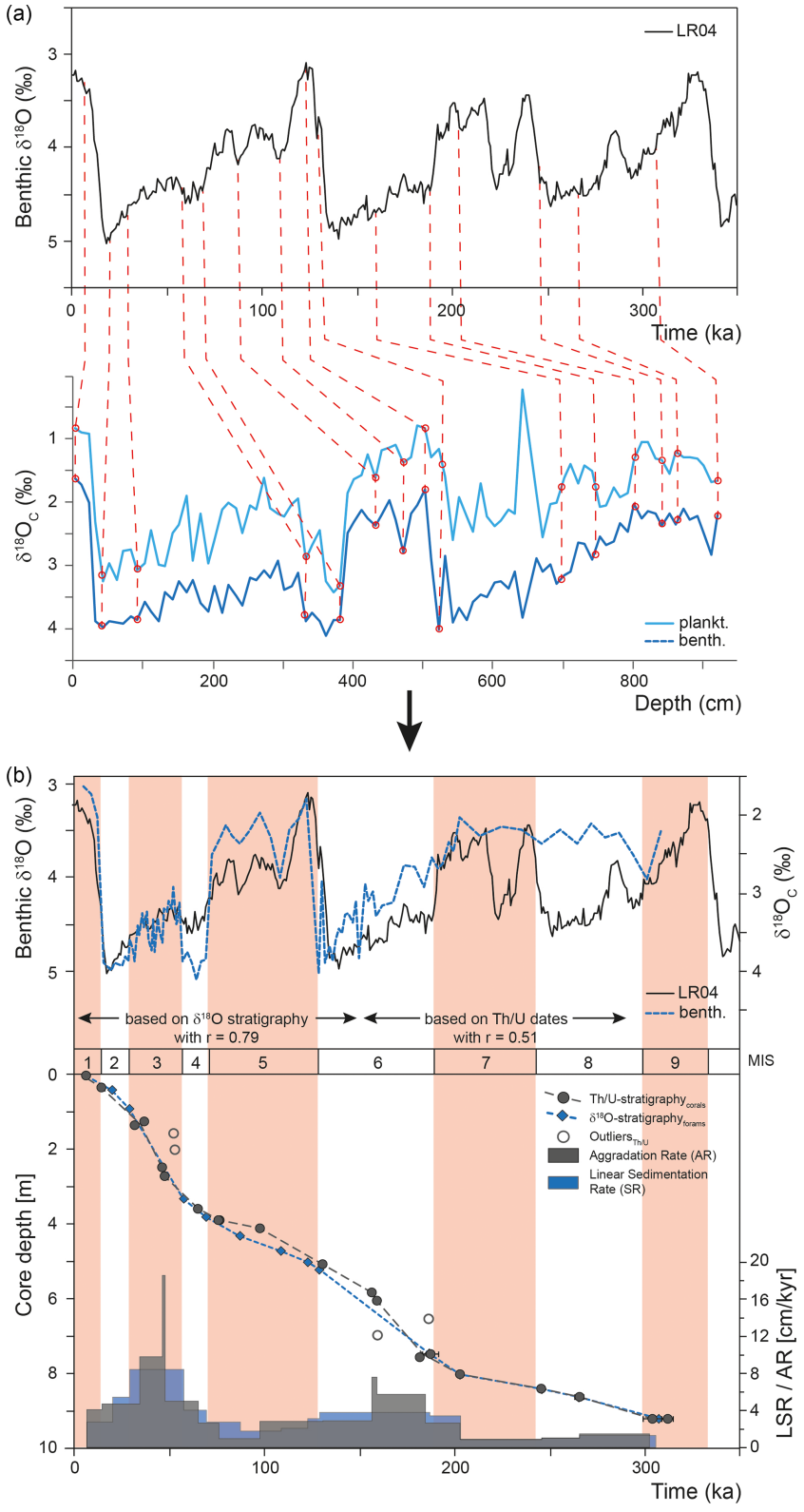

Figure 4. **(a)** Correlation pointers (see Table 3) between the LR04 benthic δ^{18}O stack of Lisiecki and Raymo (2005) and the benthic (*L. lobatula*) and planktonic (*G. bulloides*) δ^{18}O record of MD13-3462G. **(b)** The δ^{18}O stratigraphy has good correlation for the younger part (0–150 ka, $r = 0.79$, $p<0.001$), but the lower part (>150 ka), which is based on the U-series CWC dates, has a weak correlation ($r = 0.51$, $p<0.009$). The comparison between the U-series- and δ^{18}O-stratigraphy-based age–depth correlations indicates good coherence. The resulting δ^{18}O-stratigraphy-based linear sedimentation rate (LSR) may serve as an indication for changes in the sedimentary regime but shows similar values and/or trends as the CWC-age-based aggradation rate (AR), with higher rates during MIS 3, MIS 6, and late MIS 7. Marine Isotope Stages (MISs) follow boundaries defined by the LR04 stack (Lisiecki and Raymo, 2005).

Table 1. Radiocarbon ages of epibenthic foraminifera (species selected: *Lobatula lobatula*, *Cibicides refulgens*, and *Discanomalina coronata*). Ages are corrected for a reservoir age of 390 ± 80 years (Siani et al., 2000).

Lab ID	Depth (cm)	^{14}C age (BP)	± 1σ	2σ lower (cal yr BP)	2σ upper (cal yr BP)	2σ median (cal yr BP)
ETH-87743	2	5777	25	5580	5920	5760
ETH-87744	37	22 811	78	25 970	26 530	26 220
ETH-87745	87	27 587	124	30 730	31 160	30 950

Table 2. Uranium-series isotope measurements (U / Th) carried out on 24 coral fragments. All errors are 2σ of the mean analytical uncertainty. Ratios were determined using a Th–U spike calibrated to a secular equilibrium reference material (HU-1 at the IUP). Uncorrected, closed-system age was calculated using the decay constants of Jaffey et al. (1971) for ^{238}U and Cheng et al. (2000) for ^{230}Th and ^{234}U. Ages are reported relative to the date of analysis from the year 2017 (IUP-8500 to IUP-8507) and the year 2018 (other samples), and they do not include uncertainties associated with decay constants. [1] Coral species: *M*: *Madrepora oculata*; *D*: *Desmophylum pertusum*. [2] Ages corrected for the contribution of initial ^{230}Th based on an estimated seawater (^{230}Th / ^{232}Th) activity ratio of 8 ± 4. [3] Typical $\delta^{234}U_i$ reconstructed from corals for the past 30 kyr range between 135 and 155 (Chen et al., 2016). [4] Compared to the present-day seawater value of 146.8 ± 0.1 ‰, possibly indicative of U-series open-system behaviour. [5] Samples containing strong residual amounts of non-carbonate contamination, leading to high ^{232}Th concentrations and thus age corrections. [a] Replicate of IUP-8504; [b] replicate of IUP-8507.

Lab ID	Depth (cm)	S[1]	Age (ka)	±	Age[(2)] (ka)	±	^{238}U (µg g^{-1})	±	^{232}Th (ng g^{-1})	±	δ^{234}U (‰)	±	$\delta^{234}U_i^3$ (‰)	±
IUP-8500	3	*M*	6.34	0.029	6.32	0.030	4.3377	0.00037	0.4311	0.00140	147.22	0.66	149.88	0.67
IUP-8501	36	*D*	14.31	0.047	14.30	0.049	3.4367	0.00012	0.3254	0.00084	145.33	0.64	151.33	0.67
IUP-10994	126	*D*	37.16	0.085	36.70	0.25	3.8667	0.00013	7.166	0.01328	121.99	0.51	135.30	0.57
IUP-10995	136	*D*	35.53	0.10	31.9	1.3	3.4727	0.00015	36.120[5]	0.06103	126.57	0.46	138.49	0.73
IUP-8503	158	*D*	52.57	0.19	52.24	0.22	3.7330	0.00013	4.8320	0.01200	123.72	0.83	143.41	0.96
IUP-9310	201	*D*	53.07	0.12	53.04	0.13	2.6348	0.00008	0.3418	0.00059	126.01	0.45	146.39	0.53
IUP-10996	248	*D*	46.33	0.12	46.20	0.13	3.5899	0.00012	1.8802	0.0029	122.48	0.60	139.53	0.69
IUP-10997	272	*D*	47.57	0.11	47.49	0.12	3.6971	0.00013	1.1538	0.0022	121.93	0.47	139.42	0.54
IUP-10998	360	*M*	65.39	0.17	64.96	0.28	3.5499	0.00014	6.0720	0.0084	114.78	0.46	137.87	0.56
IUP-8504	390	*D*	76.44	0.29	76.43	0.29	3.6896	0.00011	0.1328	0.00039	115.92	0.67	143.86	0.84
IUP-9183[a]	390	*D*	75.66	0.20	75.65	0.17	3.7004	0.00016	0.1763	0.00046	117.75	0.49	145.83	0.61
IUP-9312	412	*D*	97.58	0.23	97.54	0.24	3.6265	0.00012	0.4572	0.00069	112.50	0.61	148.21	0.81
IUP-9313	507	*D*	130.7	0.45	130.7	0.46	3.4073	0.00015	0.3844	0.00072	105.96	0.85	153.30	1.25
IUP-10999	583	*D*	156.48	0.74	156.38	0.74	3.4985	0.00014	1.3288	0.0024	91.46	0.53	142.19	0.87
IUP-10100	604	*D*	159.17	0.69	159.13	0.69	3.5045	0.00013	0.6366	0.0011	92.98	0.55	145.69	0.90
IUP-10101	654	*D*	186.50	0.87	186.48	0.87	3.7106	0.00013	0.3339	0.00063	84.77	0.44	143.48	0.81
IUP-10102	697	*M*	159.76	0.52	159.65	0.52	4.3503	0.00017	1.9141	0.0027	87.58	0.38	137.42	0.62
IUP-8505	748	*D*	194.8	1.40	187.5	4.2	3.5659	0.00220	102.38[5]	0.27000	95.01	0.84	161.40[4]	2.40
IUP-9184	756	*D*	181.9	0.79	181.9	0.78	2.8694	0.00013	0.6018	0.00099	102.72	0.79	171.74[4]	1.40
IUP-10103	801	*D*	203.07	0.98	202.84	0.98	2.8444	0.00010	2.6095	0.0036	85.04	0.55	150.74	1.05
IUP-10104	840	*D*	245.7	1.50	245.70	1.5	3.0611	0.00011	0.2657	0.00048	78.14	0.41	156.32	1.03
IUP-9314	862	*D*	265.7	2.10	265.7	2.4	3.4662	0.00018	0.6693	0.00150	70.40	1.10	149.10	2.60
IUP-8507	921	*D*	304.2	4.80	304.2	4.9	3.0370	0.00012	0.1176	0.00044	63.32	0.68	149.60	2.60
IUP-9185[b]	921	*D*	312.1	3.40	312.1	3.0	3.3567	0.00016	0.2789	0.00061	58.58	0.77	141.50	2.20

presents typical interglacial and glacial δ^{18}O values of the Alboran Sea for both planktonic (<1 ‰ and ∼3 ‰) and benthic (∼1.5 ‰ and ∼4‰) foraminifera (e.g. Cacho et al., 1999, 2006; Stalder et al., 2015). Therefore, low planktonic and benthic δ^{18}O values correspond to interglacial periods, whilst high planktonic and benthic δ^{18}O values correspond to the two last glacial periods (Figs. 3 and 4).

4.2 Sediment characterization

The sediment in core MD13-3462G consists mostly of macrofaunal remains (essentially corals and bryozoans) embedded in a clay- to silt-sized carbonate–siliciclastic matrix. No important variation in the matrix sediment is observed throughout the core. Total organic carbon content in the sediment varies between 0.16 wt % and 1.13 wt % (Fig. 5). The highest TOC value is measured during late MIS 3 (1.13 wt %), whilst the lowest is recorded during MIS 8 (0.16 wt %; Fig. 5). The most important shifts to higher TOC

Table 3. Correlation pointers between sediment depth and time based on the benthic δ^{18}O record of core MD13-3462G and the benthic LR04 stack of Lisiecki and Raymo (2005) for main Marine Isotope Stage (MIS) boundaries. The Pearson's correlation coefficient (r) between the two records is 0.65 ($p<0.001$). Due to possibly unidentified hiatuses the linear sedimentation rate (LSR) should not be considered absolute but may serve as guidance to indicate changes in the sedimentary regime.

Depth (cm) of core MD13-3462G	Time (ka) of LR04 stack	LSR (cm ka^{-1})	
4	6.3	2.8	Top marker
42	20.0	5.5	MIS 2 peak
91	29.0	8.5	MIS 2/3
333	57.5	4.1	MIS 3/4
381	69.5	2.8	MIS 4/5
431	87.2	1.8	MIS 5.2 peak
472	108.9	2.2	MIS 5.4 peak
501	122.8	3.2	MIS 5.5 peak
522	129.1	3.9	MIS 5/6
697	159.7	3.5	Th/U date
802	203.1	0.9	Th/U date
841	245.8	1.1	Th/U date, MIS 7/8
862	265.6	1.4	Th/U date
920	307.5		Bottom marker, MIS 8/9

values are observed during MIS 5, MIS 3, and at the transition between MIS 2 and MIS 1 (Fig. 5). The sediment samples are further characterized by low hydrogen index values (<300 mg HC g^{-1} TOC; Fig. 6), indicating that the organic matter is oxidized and essentially of terrestrial origin (Espitalié et al., 1985).

The mean sortable silt grain size of the siliciclastic fraction ($\overline{SS}$) varies between ca. 19 and ca. 26 µm (Fig. 5). Overall, a decrease in $\overline{SS}$ marks the passage from interglacial to glacial periods. This is particularly noticeable at the transition from MIS 7 to MIS 6, when $\overline{SS}$ decreases abruptly from approximately 25 to 19 µm (Fig. 5). Conversely, an increasing trend is observed from ca. 550 to ca. 375 cm depth, corresponding to the passage from the later phases of MIS 6 to the end of MIS 5 (Fig. 5).

4.3 Stable carbon isotopes and elemental geochemistry

The range of δ^{13}C values of the planktonic *G. bulloides* goes from −2.2 ‰ at 12 cm to −0.5 ‰ at 292 cm, whereas that of the benthic *L. lobatula* goes from 0.9 ‰ at 872 cm to 1.8 ‰ at 362 (Fig. 5). The planktonic δ^{13}C record has higher variability compared to the benthic δ^{13}C record (Fig. 5). During MIS 6, the benthic δ^{13}C is relatively high (ca. 1.5 ‰), whilst the planktonic δ^{13}C record fluctuates between −0.6 ‰ and −1.5 ‰. A decrease in the planktonic δ^{13}C record (from −0.7 ‰ to −1.5 ‰) marks the middle of MIS 5. In contrast, the benthic δ^{13}C remains stable and low (ca. 1.2 ‰) throughout MIS 5 (Fig. 5). The passage from MIS 4 to MIS 3 is characterized by a shift from the low planktonic δ^{13}C recorded during MIS 4 (−1.5 ‰) to higher planktonic δ^{13}C (−0.5 ‰). Conversely, benthic δ^{13}C values shift from high (1.8 ‰) to lower values (1.3 ‰). The passage from MIS 2 to MIS 1 is marked by a sharp decrease in planktonic and benthic δ^{13}C (from −1.2 ‰ to −2.2 ‰ and from 1.8 ‰ to 1.0 ‰, respectively). The last two glacial intervals, in particular MIS 4, are overall marked by more negative Δ^{13}C values than during interglacials (Fig. 4). Variations in Si/Al are more marked during MIS 7 and the last glacial period in comparison with the more stable values recorded during MIS 6 and MIS 5. The transitions from MIS 7 to MIS 6 and from MIS 5 to MIS 4 are characterized by fluctuating Si/Al values (Fig. 5).

4.4 Macrofauna

The major macrofaunal fragments present in core MD13-3462G are scleractinian corals, bryozoans, brachiopods, and bivalves (Figs. 3 and 7). Sea urchins, gastropods, serpulids, and gorgonian fragments are more sporadically distributed. Although the dominant coral species in the core is *D. pertusum*, it is replaced in the upper 20 cm by *M. oculata* (Figs. 3 and 7). A third and solitary species, *Desmophyllum dianthus*, is scarcely distributed (Fig. 3). Higher CWC content is observed during interglacial periods (22.2 vol % average), whilst lower content characterizes glacial periods (14.5 vol % average) (Fig. 3). However, coral content shows an uneven distribution during MIS 3, with a range of values from less than 10 vol % to ca. 27 vol % (Fig. 3). Mound aggradation rates ranging between 5 and 18 cm kyr^{-1} during MIS 3 and early MIS 6 are well in coherence with the linear sedimentation rate based on the foraminifera δ^{18}O stratigraphy of the background sediment (Fig. 4b). In contrast, lower mound aggradation rates characterize MIS 5 (ca. 2 cm kyr^{-1}) together with MIS 1, 2, and 4 (ca. 4 cm kyr^{-1}) (Fig. 4b).

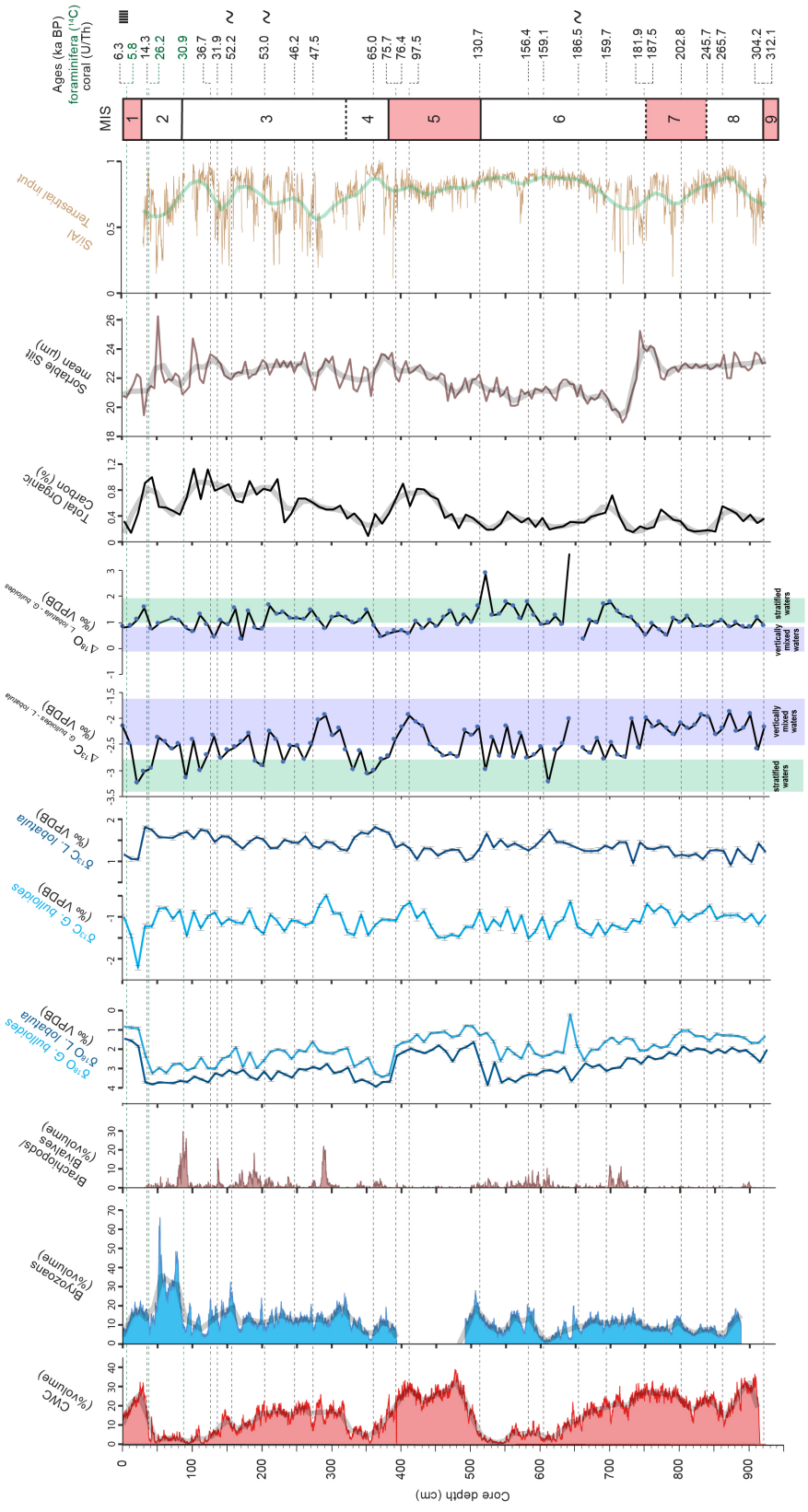

Figure 5. Planktonic (*G. bulloides*) and benthic (*L. lobatula*) δ^{13}C records, Δ^{13}C (δ^{13}C *G. bulloides* – δ^{13}C *L. lobatula*) and Δ^{18}O (δ^{18}O *L. lobatula* – δ^{18}O *G. bulloides*) records, total organic carbon content (%), mean grain size of the sortable silt fraction (the 10–63 µm grain size range, expressed in µm; McCave et al., 2006), and the $\log_{10}$ silica (Si) aluminium (Al) normalized ratio. Smoothed curves are indicated by the shaded curves. The planktonic (*G. bulloides*) and benthic (*L. lobatula*) δ^{18}O records (‰VPDB) are provided as supporting information.

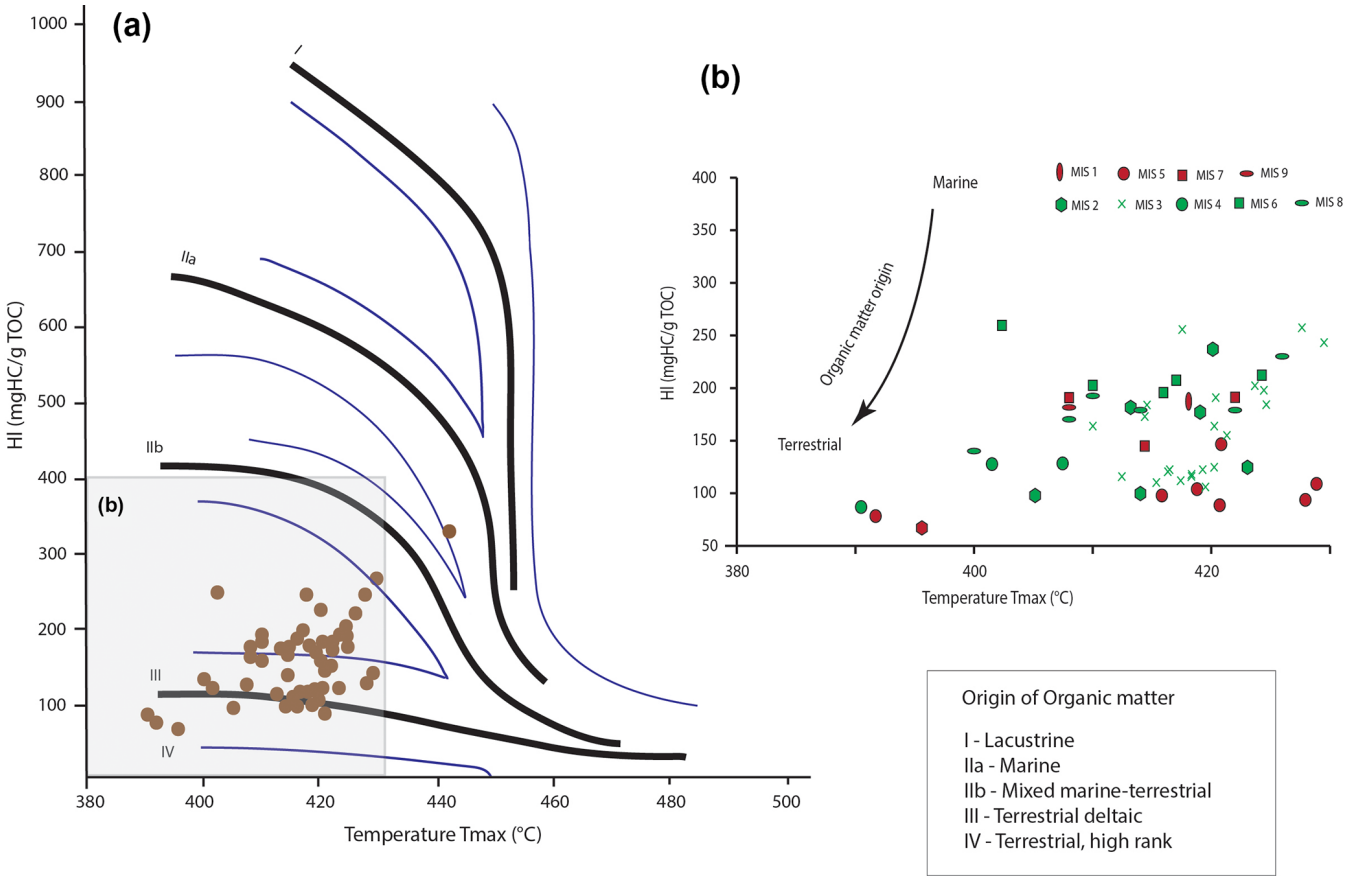

Figure 6. **(a)** Hydrogen index (HI; mgHC g^{-1} TOC) vs. T_{max} (°C) obtained by Rock-Eval6 pyrolysis. **(b)** Close-up. The organic matter origin becomes more terrestrial with decreasing HI values.

In total 23 genera of bryozoans were identified. *Buskea dichotoma* is by far the dominant bryozoan species (Fig. 8). Accessory species and genera are mainly represented by *Reteporella sparteli*, *Tubuliporina* sp., and *Palmiskenea* sp. Bryozoan content varies in general between 10 vol % and 20 vol % (Fig. 3). Very high content is, however, observed during MIS 2, reaching nearly 70 vol %. The fragments, although delicate and fragile, are well-preserved, large-sized, and unworn (Fig. 7). Bryozoans are absent during most of MIS 5. This absence corresponds to the time interval when coral content is the most important (Fig. 3). Conversely, the maximum abundance of bryozoans during MIS 2 correlates with a minimum in coral content (Fig. 3).

Brachiopods are mainly represented by the co-occurrence of the species *Gryphus vitreus* and *Terebratulina retusa* (Fig. 7). These two brachiopods are regularly associated with the bivalve *Bathyarca pectunculoides* (Fig. 7). These three invertebrates have been formerly reported from Mediterranean CWC environments. *G. vitreus* and *T. retusa* are also recorded from Pleistocene CWC deposits from Rhodes, Greece (Bromley, 2005), whilst *B. pectunculoides* was found at the Santa Maria di Leuca CWC province (Mastrototaro et al., 2010; Negri and Corselli, 2016). *G. vitreus* was also found associated with "white corals" between 235 and 255 m depth off the coast of the Hyères Islands, France (Emig and Arnaud, 1988). Although fragile, the shells are well-preserved (Fig. 7). The brachiopods and bivalves concentrate as layers and demonstrate a non-continuous distribution (Figs. 3 and 7). They reach their highest abundance during glacial periods, in particular at the end of MIS 3 (30 vol % at 80 cm). Brachiopods and bivalves are completely absent during the last two interglacial periods (Fig. 3).

4.5 Benthic foraminiferal assemblages

Shannon diversity ranges between ca. 2.8 at 652 cm and 3.6 at 782 cm (Fig. 8). High Shannon diversity values between 3.4 and 3.6 are recorded during interglacial periods (Fig. 8). The lowest Shannon diversity values (between 2.8 and 3.0) are associated with glacial periods (Fig. 8). A total of 166 benthic foraminifera species were recognized (see the Supplement). The most abundant species are *Bolivina spathulata*, *Bulimina marginata*, *Bulimina striata*, *Cassidulina laevigata*, *D. coronata*, *Gavelinopsis praegeri*, *Globocassidulina subglobosa*, *Hyalinea balthica*, *L. lobat-*

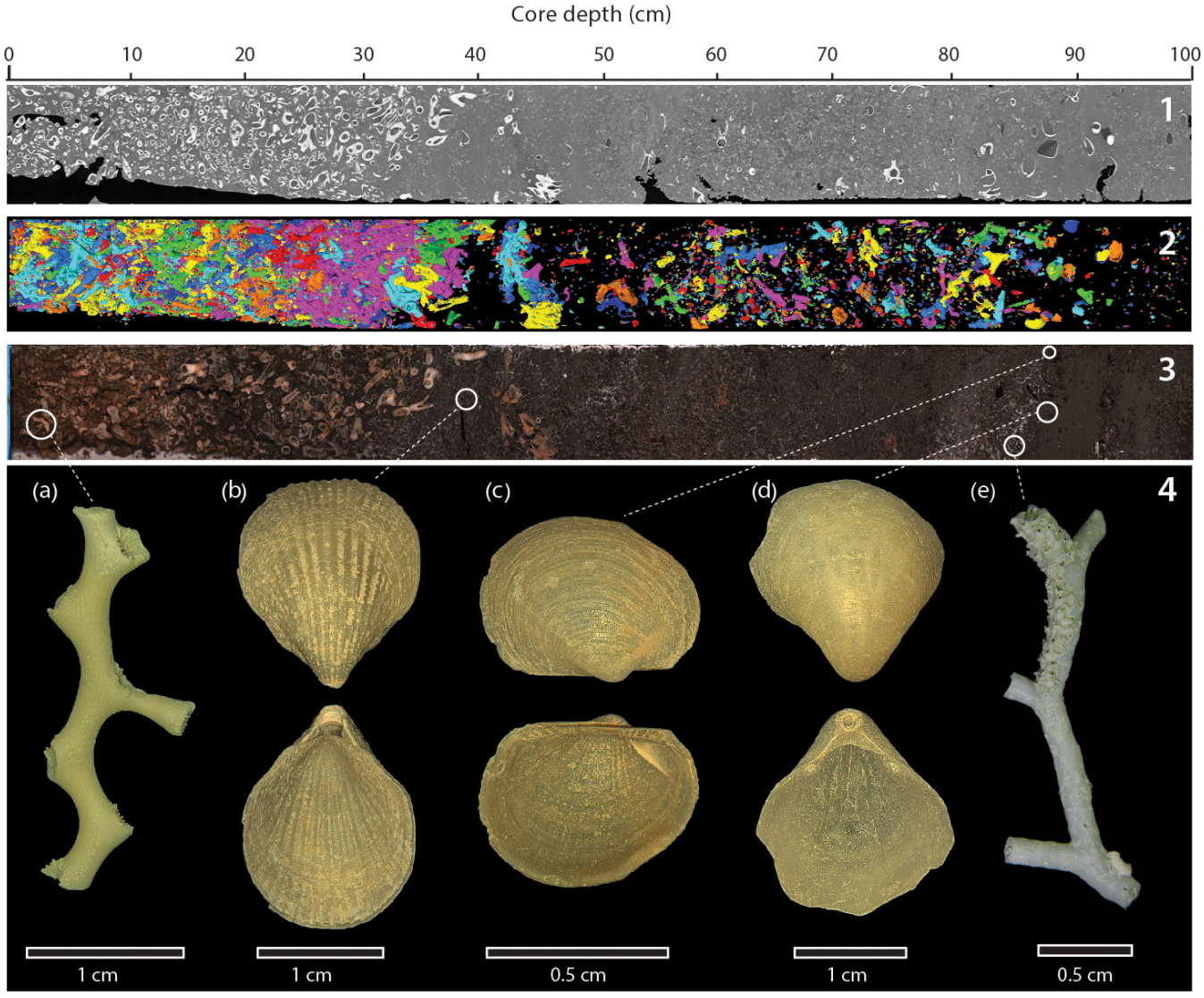

Figure 7. Example of a sediment core section showing the main macrofaunal components (section 1, 0–100 cm). (1) X-ray computed tomography imagery. (2) Three-dimensional reconstruction of coral fragments performed on X-ray CT images. (3) Split-core high-resolution image. (4) Main macrofaunal components: **(a)** the coral *Madrepora oculata*, **(b)** the brachiopod *Terebratulina retusa*, **(c)** the bivalve *Bathyarca pectunculoides*, **(d)** the brachiopod *Gryphus vitreus*, and **(e)** the bryozoan *Buskea dichotoma*.

ula, *Miliolinella subrotunda*, *Trifarina angulosa*, and *Uvigerina mediterranea* (Fig. 9).

The three Buliminid species *Bulimina aculeata*, *B. marginata*, and *B. striata* demonstrate the same distribution trends and were thus grouped together as *Bulimina* spp. (Fig. 8). All Miliolids were grouped together for the same reason. The species *M. subrotunda* makes up more than half of the total abundance of the Miliolid group with an average contribution of ca. 53.4 %. The abundances of all important species are given in Fig. 8. The opportunistic infaunal *Bulimina* spp. show maximum abundances during interglacial periods (ca. 18 %) and minimum abundances during glacial periods (ca. 2 %; Fig. 8). *U. mediterranea* follows a similar distribution as Buliminids, with peak abundances corresponding to interglacial periods (Fig. 8). Relative to *Bulimina* spp., *U. mediterranea*, and *G. subglobosa*, the infaunal *T. angulosa* and the epifaunal *D. coronata* are the least abundant during the last two interglacials (between ca. 1 % and 5 %), whilst they are the most abundant during glacial periods, with peak abundances reached during MIS 4 for *D. coronata* (ca. 30 %; Fig. 8). Abundances of Miliolids (5 %–22 %), *L. lobatula* (3 %–17 %), and *C. laevigata* (3 %–17 %) are relatively high throughout the entire core (Fig. 8), although Miliolids show higher abundances during glacials (ca. 20 %). The highest numbers of *C. laevigata* are recorded during glacial periods (ca. 20 %), whilst minimum abundances occur during

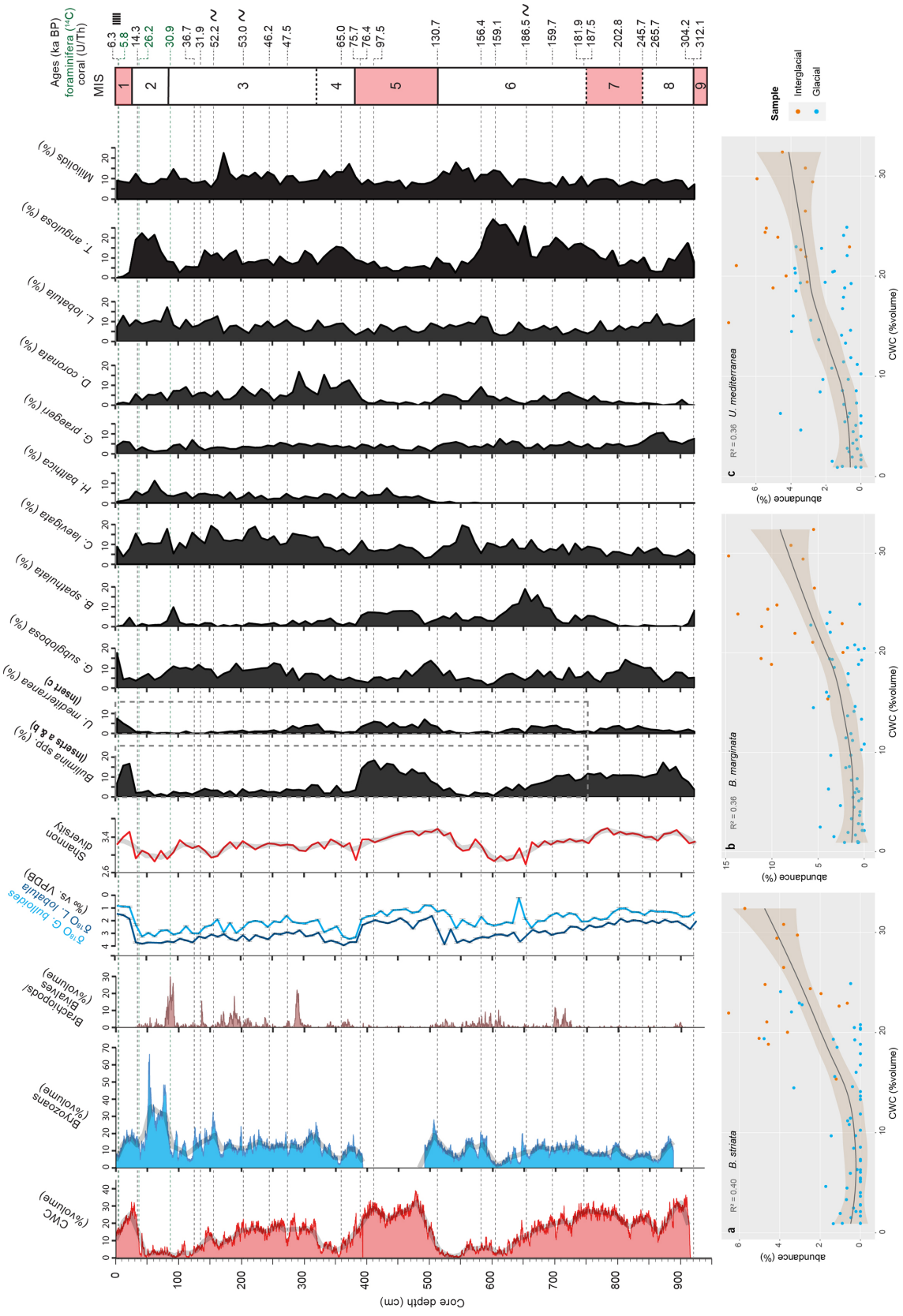

Figure 8. Distribution of main benthic foraminifera species (relative abundances) and benthic foraminiferal Shannon diversity. The planktonic (*G. bulloides*) and benthic (*L. lobatula*) δ^{18}O records (‰, VPDB) are provided as supporting information. Panels **(a)**, **(b)**, and **(c)**: relative abundance of *B. striata*, *B. aculeata*, and *U. mediterranea* vs. CWC content (vol %) over the last two interglacial–glacial cycles (dashed grey rectangles). Shaded brown outlines represent the locally weighted regression (Cleveland and Devlin, 1986).

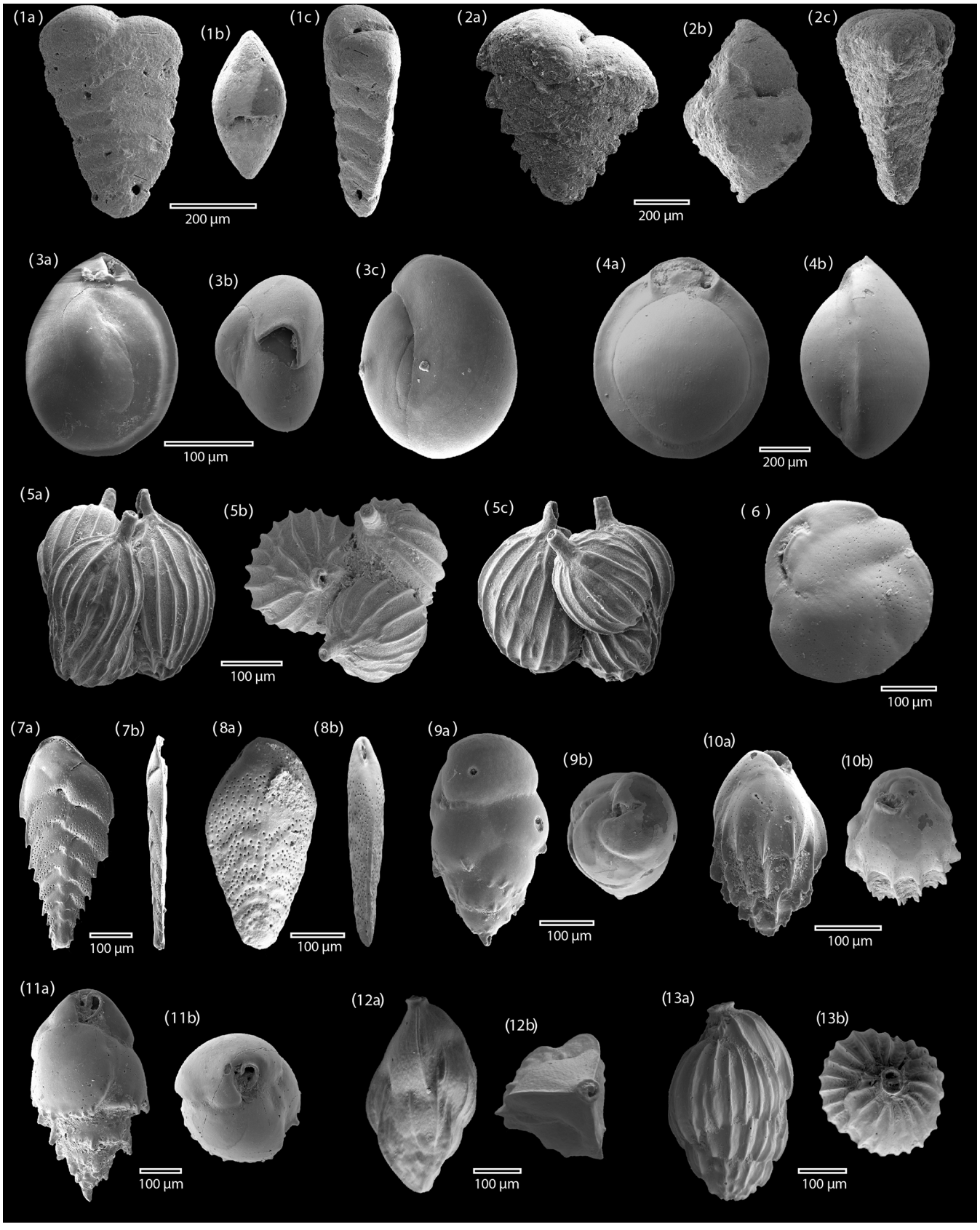
(1a)
(1b)
(1c)
200 µm
(2a)
(2b)
(2c)
200 µm
(3a)
(3b)
(3c)
100 µm
(4a)
(4b)
200 µm
(5a)
(5b)
100 µm
(5c)
(6)
100 µm
(7a)
(7b)
100 µm
(8a)
(8b)
100 µm
(9a)
(9b)
100 µm
(10a)
(10b)
100 µm
(11a)
(11b)
100 µm
(12a)
(12b)
100 µm
(13a)
(13b)
100 µm

Figure 9.

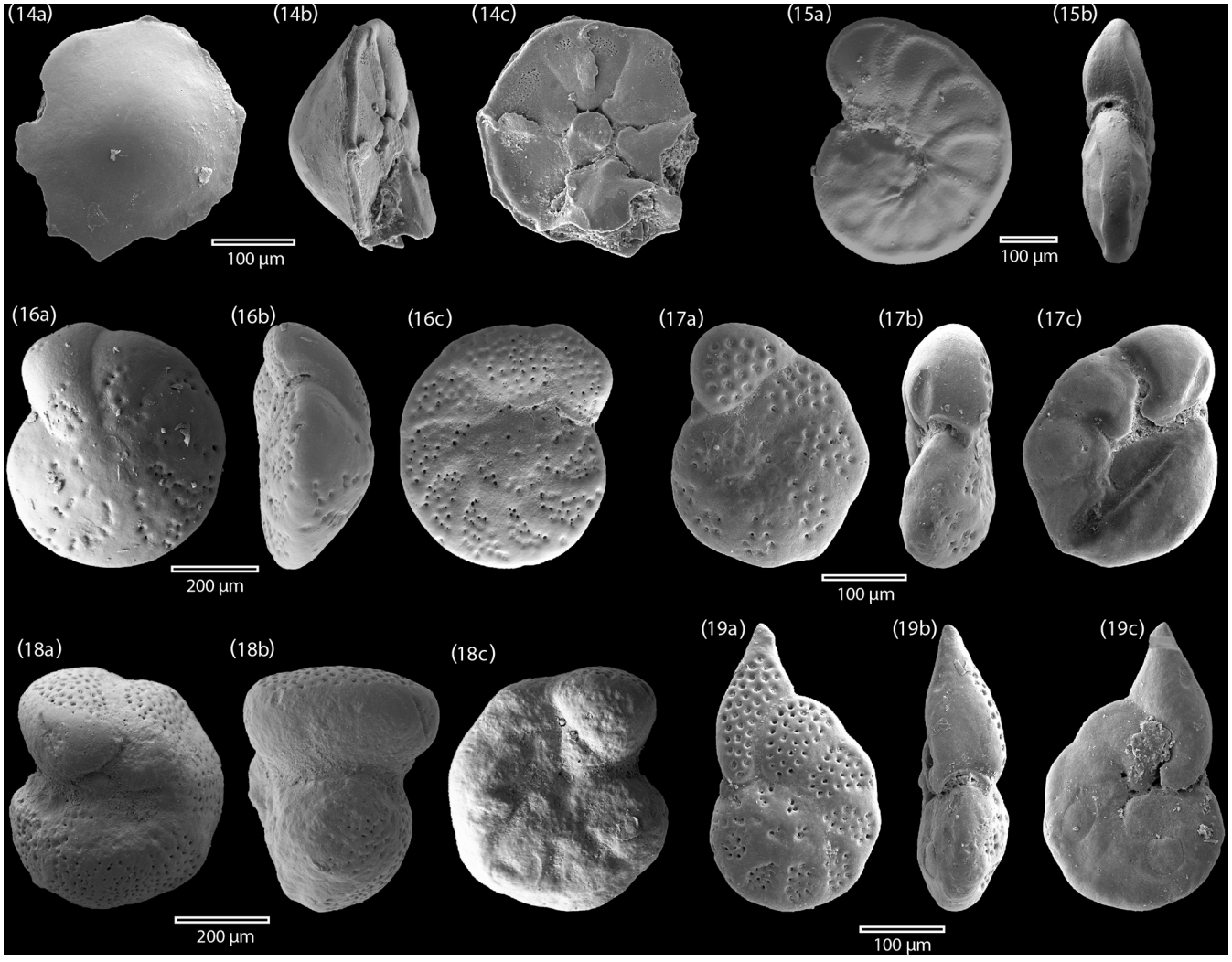

Figure 9. Scanning electron microscope (SEM) images of characteristic benthic foraminifera from core MD13-3462G. (1) *Spiroplectammina wrightii* (Silvestri, 1903) – a: side view, b: apertural view, c: peripheral view. (2) *Spirorutilus carinatus* (Cushman, 1921) – a: side view, b: apertural view, c: peripheral view. (3) *Miliolinella subrotunda* (Montagu, 1803) – a: side view 1, b: apertural view, c: side view 2. (4) *Pyrgo anomala* (Schlumberger, 1891) – a: side view, b: side view. (5) *Lagena* sp. (Walker and Jacob, 1798) – a: side view 1, b: apertural view, c: side view 2. (6) *Cassidulina laevigata* (d'Orbigny, 1826), side view. (7) *Bolivina alata* (Seguenza, 1862) – a: lateral view, b: peripheral view. (8) *Bolivina spathulata* (Williamson, 1858) – a: lateral view, b: peripheral view. (9) *Bulimina aculeata* (d'Orbigny, 1826) – a: lateral view, b: apertural view. (10) *Bulimina striata* (d'Orbigny, 1826) – a: lateral view, b: apertural view. (11) *Bulimina marginata* (d'Orbigny, 1826) – a: lateral view, b: apertural view. (12) *Trifarina angulosa* (Williamson, 1858) – a. lateral view, b. apertural view. (13) *Uvigerina mediterranea* (Hofker, 1932) – a: lateral view, b: apertural view. (14) *Gavelinopsis praegeri* (Heron-Allen and Earland, 1913) – a: spiral side, b: peripheral view, c: umbilical side. (15) *Hyalinea balthica* (Schröter, 1783) – a: spiral side, b: peripheral view. (16) *Lobatula lobatula* (Walker and Jacop, 1798) – a: spiral side, b: peripheral view, c: umbilical side. (17) *Discanomalina vermiculata* (d'Orbigny, 1839) – a: spiral side, b: peripheral view, c: umbilical side. (18) *Discanomalina coronata* (Parker and Jones, 1865) – a: spiral side, b: peripheral view, c: umbilical side. (19) *Discanomalina japonica* (Asano, 1951) – a: spiral side, b: peripheral view, c: umbilical side.

interglacials (3 % during MIS 5). The epifaunal *G. praegeri* is homogeneously distributed in contrast to *H. balthica*, which first appears in the core at the onset of MIS 5, reaching maximum abundances during MIS 2 (ca. 11 %; Fig. 8). The infaunal *B. spathulata* is the most abundant during MIS 6 (ca. 20 %) and reaches approximately 10 % during interglacial periods (MIS 9, MIS 7 and MIS 5; Fig. 8).

5 Discussion

5.1 Build-up heterogeneity among Mediterranean coral mounds

5.1.1 Variability of coral mound build-up within the western Mediterranean

Long-term coral mound formation at the location of core MD13-3462G took place during both interglacial and glacial periods (Fig. 4b). The highest mound aggradation rates of ca. 6 and 10 cm kyr^{-1} are respectively reached during the middle of MIS 6 and MIS 3, with a short peak of 18 cm kyr^{-1} during MIS 3. Mound aggradation rates do not exceed ca. 4 cm kyr^{-1} during interglacial periods and generally range between 1 and 2 cm kyr^{-1} (Fig. 4b). These rates are comparable to inactive reefs in the Porcupine Seabight (<5 cm kyr^{-1}; Frank et al., 2011) and are below the 15 cm kyr^{-1} threshold set by Frank et al. (2009) for active CWC reef and mound formation, thus suggesting that CWCs did not thrive at the site of core MD13-3462G but rather developed under stressful environmental conditions. The planktonic and benthic δ^{18}O values recorded for the last two interglacial and glacial periods, which demonstrate typical interglacial–glacial variations (Fig. 4; Cacho et al., 1999; Lisiecki and Raymo, 2005; Cacho et al., 2006), are a clear indication that the studied mound location demonstrates a slow albeit continuous build-up history across this time period.

Mound aggradation rates for core MD13-3462G are lower than the rates of 17 and 25 cm kyr^{-1} respectively calculated for MIS 9 and 7 in the neighbouring BRI core GeoB18118-2 (Krengel, 2020) and those of 49 and 83 cm kyr^{-1} respectively calculated for MIS 7 and 5 in core GeoB18116-2 on Dragon Mound (Fig. 1c; Krengel, 2020). Similar to the very low mound aggradation rates observed during MIS 5 in core MD13-3462G (ca. 2 cm kyr^{-1}, Fig. 4b), Krengel (2020) noticed an absence of coral mound build-up during MIS 5 on BRI. With only 9.2 m accumulated over the last ca. 300 kyr against ca. 32 m for the same time period at the site of core GeoB18118-2 (Krengel, 2020), the overall mound aggradation at the site of core MD13-3462G is particularly low. This threefold difference in mound aggradation may suggest that the northern part of BRI (core MD13-3462G) was submitted to more mass-wasting events and/or erosional processes than the southern area (core GeoB18118-2; Krengel, 2020), resulting as such in an overall reduced mound build-up. However, as discussed previously, the benthic and planktonic δ^{18}O values recorded for the last two interglacial and glacial periods, together with the absence of erosional features downcore, allow us to dismiss this hypothesis. Krengel (2020) also observed that core GeoB18118-2 was in stratigraphic order and only showed minor signs of erosional processes. MD13-3462G (this study) and GeoB18118-1 (Krengel, 2020) are both situated on the crest of BRI at 327 and 332 m depth, respectively, at a distance of ca. 1.3 km (Fig. 1c). Therefore, the observed differences in the timing and rates of long-term mound build-up at BRI are likely driven by local rather than regional and/or basin-wide environmental variability. We propose that disparities in hydrodynamic regimes could lead to reduced food supply and/or low sediment input at the northern part of the ridge where core MD13-3462G was recovered. Supplementary investigations for both cores using bottom current proxies are, however, needed to test this hypothesis. A number of studies have demonstrated that the EMCP and West Melilla Coral Province experienced a rapid phase of mound build-up during the Bølling–Allerød interstadial and the early Holocene (Fink et al., 2013; Stalder et al., 2015; 2018; Wang et al., 2019; Wienberg, 2019; Fentimen et al., 2020a; Krengel, 2020) with mound aggradation rates varying between 75 and 420 cm kyr^{-1}. Similar mound aggradation rates between 44 and 203 cm kyr^{-}1 were calculated by Corbera et al. (2021) at the Cabliers Mound Province. However, in contrast with these observations, mound deposits recovered within core MD13-3462G do not demonstrate such a rapid build-up phase (Fig. 4b). We hypothesize that this deviation from the Alboran Bølling–Allerød to early Holocene mound build-up trend is further evidence that the coral communities situated at the northern part of BRI developed under unfavourable environmental conditions.

In the South Cabliers Mound Province, Corbera et al. (2021) identified four mound formation phases covering the last 400 kyr spread between MIS 9, 7, 6, and 5 at rates of 4, 5, 3.5, and 20 cm kyr^{-1}, respectively, whereas long-term mound build-up at the Tunisian Coral Mound Province in the central Mediterranean essentially took place during MIS 2 at rates of ca. 20 cm kyr^{-1} (Corbera et al., 2022). These different mound build-up phases were separated by periods of mound stagnation (Corbera et al., 2021, 2022). The contrasting observations made at the Cabliers Mound Province, Tunisian Coral Mound Province, Dragon Mound, and BRI (Krengel, 2020; Corbera et al., 2021, 2022, this study) suggest that, together with local discrepancies at BRI, the timing of long-term mound build-up in the western and central Mediterranean is not concurrent and does not follow a clear interglacial–glacial pattern as in the North Atlantic (Dorschel et al., 2005; Rüggeberg et al., 2007; Frank et al., 2009, 2011; Matos et al., 2015, 2017). The temporal distribution of western and central Mediterranean CWC mounds is rather comparable to mounds situated off the coasts of Angola and Mauritania, where mound build-up took place during both interglacial and glacial periods (Wienberg and Titschack, 2016;

Wefing et al., 2017; Wienberg et al., 2018). Overall, the striking disparity in the timing of mound build-up across the western and central Mediterranean hints at strong differences in regional and local environmental forcing.

5.1.2 Glacial mound build-up: a recurrent Mediterranean trend?

Core MD13-3462G provides the first record of consistent coral growth during the last glacial period in the EMCP and more generally in the Alboran Sea (Fig. 3). Previous observations made by Krengel (2020) at BRI and Dragon Mound evidence very scarce occurrences during MIS 6, with two corals dated at 145.7 and 142.5 ka at BRI and another individual dated at 171.9 ka at Dragon Mound. The Cabliers Mound Province is also characterized by an absence of CWCs during the last glacial, despite demonstrating a phase of mound build-up during MIS 6 (Corbera et al., 2021). Thus, the last glacial occurrence of CWCs in core MD13-3462G stands out, all the more so given that mound aggradation rates reach their highest values during this time (Fig. 4b). This observation contrasts with the complete absence of last glacial coral occurrences in the neighbouring core GeoB18118-1 investigated by Krengel (2020) and demonstrates once again the important heterogeneity in the timing of long-term coral mound build-up along BRI and more generally in the Alboran Sea.

Last glacial occurrences of CWCs and mound aggradation rates of 18.3–21.6 cm kyr^{-1} have recently been reported at the Tunisian Coral Mound Province in the central Mediterranean (Corbera et al., 2022). Coral mound formation is essentially concentrated during MIS 2 (Corbera et al., 2022), unlike at the northern part of BRI (core MD13-3462G) where the most important mound build-up phase occurred during MIS 3 (Fig. 4b). Corbera et al. (2022) argue that increased productivity was a main driver behind this MIS 2 mound formation phase. Likewise, coral growth during the last glacial has been reported from the Gulf of Cádiz and is also suggested to be promoted by increased paleo-productivity linked to strengthened aeolian dust import (Wienberg et al., 2009). Thus, coral growth during the last glacial period spans from the Gulf of Cádiz to the western (EMCP) and central (Tunisian Coral Mound Province) Mediterranean and appears to be a recurrent pattern. The benthic and planktonic foraminiferal $\delta^{18}O$ and $\delta^{13}C$ values from core MD13-3462G suggest that environmental conditions were particularly unstable during the last glacial period, as suggested by previous studies (Cacho et al., 2000; Martrat et al., 2004; Pérez-Folgado et al., 2004; Cacho et al., 2006; Bout-Roumazeilles et al., 2007). Moreover, high numbers of the infaunal benthic foraminifera *G. subglobosa* and *C. laevigata* (Fig. 8) would indicate that MIS 3 was marked by phases of increased productivity (Schmiedl and Mackensen, 1997; Martins et al., 2006), hence similar to the environmental conditions during the last glacial at the Tunisian Coral Mound Province and Gulf of Cádiz coral mounds.

In contrast with other long-term Mediterranean coral mound records (Krengel, 2020; Corbera et al., 2021, 2022), the mound deposits situated at the northern part of BRI (site MD13-3462G) show a high contribution of the erect cheleistome bryozoan *B. dichotoma* (Fig. 3). High abundance of this species during the Bølling–Allerød has previously been reported from the EMCP, where it reached approximately 20 % of the total macrofaunal assemblage (Stalder et al., 2015). Fentimen et al. (2020a) also documented *B. dichotoma* abundances of up to 30 vol % at the end of the last glacial period at BRI (in core MD13-3455G, see Fig. 1c). With the exception of MIS 5, the mound deposits recovered in core MD13-3462G demonstrate that *B. dichotoma* was present in numbers throughout the last 300 kyr of mound development and was particularly abundant during the last glacial (ca. 70 vol %; Fig. 3). Based on mound aggradation rates and macrofaunal content, we propose that *B. dichotoma* communities favoured mound formation at the site of core MD13-3462G, noticeably during the last glacial, by capturing fine-grained sediments in a similar way as CWCs do. As such, the investigated mound deposits stand out and may be considered a mixed *B. dichotoma*–CWC framework rather than a CWC mound per se.

5.2 Environmental controls on coral proliferation during the last two interglacial periods

During interglacial periods, benthic foraminiferal assemblages at BRI are marked by high abundances of the infaunal *Bulimina* spp., *U. mediterranea*, and to a lesser extent *B. spathulata*. Several authors describe *Bulimina* spp. as characteristic for eutrophic and dysoxic environments (Phleger and Soutar, 1973; Lutze and Coulbourn, 1984; Jorissen, 1987; Schmiedl et al., 2000). In the Mediterranean Sea, they are dominant in the vicinity of the Po River delta in the northern Adriatic Sea and close to the Rhône River delta (Jorissen, 1987; Mojtahid et al., 2009). The shallow infaunal *U. mediterranea* and the opportunistic *B. spathulata* are known to demonstrate a positive correlation with organic matter flux (De Rijk et al., 2000; Schmiedl et al., 2000; Fontanier et al., 2002, 2003; Drinia and Dermitzakis, 2010). Moreover, *Bulimina* spp. and *U. mediterranea* are reported to be able to feed on fresh but also more refractory organic matter (De Rijk et al., 2000; Koho et al., 2008; Dessandier et al., 2016). Based on these observations, the benthic foraminiferal assemblage during interglacials would support high organic matter export to the seafloor. The overall higher TOC levels during interglacials confirm that the sediment during these periods was relatively enriched in organic matter in comparison to glacial periods (Fig. 5). High abundance of the shallow infaunal *G. subglobosa* has been linked to the deposition of fresh phytodetritus on the seafloor after bloom events (Gooday, 1993; Fariduddin and Loubere, 1997; Suhr et al., 2003; Sun et al., 2006). It is typically found in high-energy (e.g. steep flanks, ridges) and well-oxygenated envi-

ronments (Mackensen et al., 1995; Milker et al., 2009), and it is a common taxon of the Alboran Platform and of CWC environments (Margreth et al., 2009; Milker et al., 2009; Spezzaferri et al., 2014). Mackensen et al. (1995) noted that *G. subglobosa* dominated in areas of the South Atlantic Ocean where the organic carbon flux did not exceed $1\,g\,m^{-2}\,yr^{-1}$. In contrast, in the Mediterranean Sea, *B. marginata* is restricted to sites with an organic carbon flux $>2.5\,g\,m^{-2}\,yr^{-1}$, whilst *B. aculeata* is associated with a flux of $3\,g\,m^{-2}\,yr^{-1}$ (De Rijk et al., 2000). The last two interglacials (MIS 7 and MIS 5) are marked by an increased abundance of *G. subglobosa* at early stages followed by a general decline. Buliminids follow a converse trend, particularly during MIS 5, with lower abundances at early stages (Fig. 8). This suggests that conditions during the later stages of interglacials became increasingly eutrophic and in turn less oxygenated at the sediment–water interface, as the consumption of organic matter led to oxygen depletion. These more environmentally stressful conditions resulted in decreased foraminiferal diversity and a proliferation of opportunistic taxa (Fig. 8). Indeed, the lower abundances of Miliolids, which are typically found in well-oxygenated environments (Murray, 2006), further confirm eutrophication coupled to lower oxygenation at the seafloor during interglacials, specifically towards the end of such periods (Fig. 8). Yet, the absence of deep infaunal benthic foraminifera (e.g. *Chilostomella* spp. or *Globobulimina* spp.) implies that seafloor oxygenation was never at a minimum, such as during the restricted intervals prior to and after sapropel events in the eastern Mediterranean (Jorissen, 1999; Schmiedl et al., 2003).

Schmiedl et al. (2010) link the high abundance of *U. mediterranea* in the Aegean Sea to humid climatic conditions and increased river runoff. Increased fluvial input has been widely linked in the eastern Mediterranean to more humid continental conditions during interglacial times in response to a northern shift of the African monsoon (e.g. Gasse, 2000; Gasse and Roberts, 2005; Osborne et al., 2008; Coulthard et al., 2013). In contrast, the Alboran Sea lies below the maximum Intertropical Convergence Zone northward position and is sheltered by the Atlas Mountains (Rohling et al., 2002; Tuenter et al., 2003; Lavaysse et al., 2009). Modern-day observations show that rainfall over the northwestern Atlas Mountains is generally associated with baroclinic activity over the North Atlantic (Knippertz et al., 2003; Braun et al., 2019). The south of the Atlas Mountains has one of the highest cyclonic activities in the Mediterranean borderlands, whilst the largest fraction of cyclones entering the Mediterranean Sea arrives from the Atlantic (Lionello et al., 2016). Pasquier et al. (2018) noticed that periods of increased input of organic matter from sediment-laden rivers occur during warm substages of the last 200 kyr. These authors relate these pluvial events to negative North Atlantic Oscillation-like conditions (Pasquier et al., 2018). The EMCP is located 50 km away from the mouth of the Moulouya River, which takes its source in the High Atlas Mountains (Snousi, 2004; Emelyanov and Shimkus, 2012; Tekken and Kropp, 2012). The basin of the Moulouya River covers approximately $54\,000\,km^2$, hence representing the largest river basin in northwestern Africa (Emelyanov and Shimkus, 2012; Tekken and Kropp, 2012). We propose that the influence of warm and moist Atlantic air masses during interglacial periods promoted warmer and more humid conditions over northwestern Africa and torrential rainfall. This would have led to a strengthening of the Moulouya River's flow rate, hence triggering episodes of important terrestrial organic matter input at BRI. These events may have in turn caused eutrophication and oxygen depletion at the seafloor, compatible with the observed benthic foraminiferal assemblages (Fig. 8).

In addition, the variations in the ventilation of the eastern Mediterranean Sea and the formation of LIW may also drive the observed benthic foraminiferal assemblages and reduced mound aggradation rates during interglacial periods. Indeed, at the EMCP Stalder et al. (2015) reported a benthic foraminiferal assemblage of similar composition as the interglacial benthic foraminiferal community within core MD13-3462G. The assemblage described by Stalder et al. (2015) also demonstrates a high abundance of *B. marginata*, *B. aculeata*, and *C. laevigata*. It coincides with periods of *D. pertusum* absence and the deposition of sapropel S1 in the eastern Mediterranean, hence suggesting that sapropel-related perturbations to the thermohaline circulation triggered oxygen depletion at the seafloor. Sapropel events have also been shown to be concurrent with coral demise in the Cabliers Mound Province, at least since sapropel 7 at the end of MIS 7 (Corbera et al., 2021), and in the southern Adriatic Sea (Taviani et al., 2019). During sapropel events, water column stratification in the eastern Mediterranean led to a dwindling of LIW formation and consequently its reduced circulation in the western Mediterranean Basin (Toucanne et al., 2012; Bahr et al., 2015; Filippidi et al., 2016). Similar to the Cabliers Mound Province (Corbera et al., 2021) and as suggested by benthic foraminiferal assemblages, oxygen depletion linked to reduced LIW circulation and important organic matter input may have resulted in unfavourable and stressful environment conditions for coral growth during interglacial periods, hence explaining the low mound aggradation rates recorded within core MD13-3462G (Fig. 4).

During interglacial periods, the high sea level and the increased evaporation in the Mediterranean led to a more important inflow of low-salinity MAW through the Strait of Gibraltar (Sierro et al., 2005). Thus, surface waters in the Alboran Sea are, in comparison to glacial periods, warmer and less dense. This is also noticed in the planktonic $\delta^{18}O$ record (Fig. 3). The enhanced MAW flow during interglacials triggers stronger Western and Eastern Alboran Gyres, resulting in better mixing and downwelling. Knowing that the Provençaux Bank and BRI are situated at relatively shallow water depths and in the path of the westward-circulating branch of the Eastern Alboran Gyre (Lanoix, 1974; Viúdez and Tintoré, 1995; Fig. 10), as well as that mixing between

surface and intermediate water masses is documented to occur down to ca. 300 m water depth (Heburn and La Violette, 1990), it is conceivable that the corals currently living at 327 m depth were bathed by or situated at the limit of mixing between surface and intermediate water masses during interglacial periods. Wang et al. (2019) suggest that the same phenomenon occurred during the Bølling–Allerød interstadial and the early Holocene. Higher input of MAW into the Alboran Sea would lead to an increased contribution of surface waters to LIW (Fig. 10) and a deepening of the pycnocline. This would promote the formation of internal waves and increase turbulence at the seafloor of BRI, as suggested by the slightly higher $\overline{SS}$ values at the end of interglacials (Fig. 5), and would have favoured coral proliferation by increasing lateral nutrient supply (Fig. 10). A better mixing of surface and intermediate water masses is suggested by the decreased $\Delta^{13}C$ and $\Delta^{18}O$ during the last two interglacial periods (Fig. 5). We suggest that increased food availability during interglacial periods may have enabled coral communities to develop despite oxygen-depleted seafloor conditions in the same way as in the oxygen minimum zones on the Angolan and Namibian margins (Hanz et al., 2019). These conditions would, however, have been detrimental for bryozoan communities.

5.3 Environmental conditions during the last two glacial periods

With the exception of MIS 8, for which the boundaries are poorly defined, glacial periods are marked by a change in macrofaunal composition with lower coral and higher bryozoan content in comparison to interglacial periods (Fig. 3). This higher bryozoan content at BRI is in tune with previous observations made at the Great Australian Bight, where bryozoan proliferation during glacial periods promoted the formation of mounds (James et al., 2000; Holbourn et al., 2002). Conversely, higher temperatures and downwelling during interglacials halted bryozoan extension at the Great Australian Bight (James et al., 2000; Holbourn et al., 2002). Rigid erect branching bryozoans such as *B. dichotoma* are known to be fragile and hence to prefer low-energy environments, being unable to withstand strong bottom currents and turbulence (Scholz and Hillmer, 1995; Bjerager and Surlyk, 2007). Eutrophic environments dominated by infaunal benthic foraminifera (e.g. *Bulimina* spp.) are unfavourable for erect bryozoans due to the high concentration of suspended food particles clogging up their feeding apparatus (Holbourn et al., 2002). Low $\overline{SS}$ values and reduced TOC content in the sediment confirm that glacial periods were marked by weaker bottom current velocities and organic matter flux (Fig. 5). The presence of brachiopod and bivalve layers dominated by the brachiopod *G. vitreus* also characterizes the glacial macrofauna (Fig. 3). This species is found between 160 and 250 m depth along the Mediterranean continental margin and thrives in areas dominated by moderate bottom currents (Emig and Arnaud, 1988). Thus, the co-occurrence of this species with bryozoans confirms that variations in sea level stand, hydrodynamics, and trophic conditions govern the change in macrofaunal dominance at BRI. Low organic matter flux during glacial periods has been related to predominantly arid conditions over North Africa, in association with a weak North African monsoon (Gasse, 2000; Sierro et al., 2005).

The reduced precipitation and retreat of vegetation would have triggered a dwindling of terrestrial input during the last glacial period at BRI, as evidenced by a generally lower Si/Al elemental ratio (Fig. 5).

Glacial benthic foraminiferal assemblages are characterized by the dominance of large epibenthic suspension-feeding foraminifera, such as *L. lobatula* and *D. coronata*, together with the infaunal *C. laevigata* (Fig. 8). This follows observations made by Stalder et al. (2018), who noticed increased abundances of *Cibicides* spp., *D. coronata*, and *C. laevigata* during glacial periods at BRI. These species share a preference for high-quality fresh marine organic matter (De Rijk et al., 2000; Milker et al., 2009; Stalder et al., 2018). *Lobatula lobatula* and *D. coronata* have been described to prefer oxygen-rich bottom waters (Linke and Lutze; 1993; Margreth et al., 2009). In the Arctic basins and Norwegian–Greenland Sea, the dominance of the epibenthic *Cibicides wuellerstorfi* (a relative of *L. lobatula*) reflects a relatively low flux of organic matter (Linke and Lutze; 1993) as this species tolerates vertical flux rates $<2\,g\,cm^{-2}\,yr^{-1}$ (Altenbach, 1989). The dominance of *L. lobatula*, *D. coronata*, *C. laevigata*, and Miliolids would thus indicate that the seafloor during glacial periods received less but higher-quality organic matter and became more oxygenated in response to the stronger influence of intermediate and deep-water masses (Fig. 10). These observations suggest that more arid conditions during glacial periods led to a reduced influence of terrestrial input on benthic communities (Fig. 10). We propose that weaker but comparatively fresher organic matter input allowed the development of CWC communities, particularly during the last glacial period, and the bryozoan *B. dichotoma*. This assumption is supported by experimental observations demonstrating how erect bryozoans essentially feed on diatoms and that suspension-feeding foraminifera use the same food sources (Winston, 1977, 1981; Best and Thorpe, 1994; Goldstein, 1999). It can be hypothesized that there may be a threshold in the quality and quantity of organic matter determining whether *D. pertusum* or *B. dichotoma* dominates the benthic environment at BRI.

Wang et al. (2019) relate low off-mound $\overline{GS}$ and high benthic foraminiferal $\delta^{13}C$ values at BRI during glacials to a dominant influence of MAW coinciding with a low sea level stand. However, whilst the benthic foraminiferal $\delta^{13}C$ values from core MD13-3462G are indeed relatively high during glacial periods, the planktonic foraminiferal $\delta^{13}C$ values do not follow the same trend (Fig. 5). The overall low $\Delta^{13}C$ values during the two last glacial periods, noticeably during

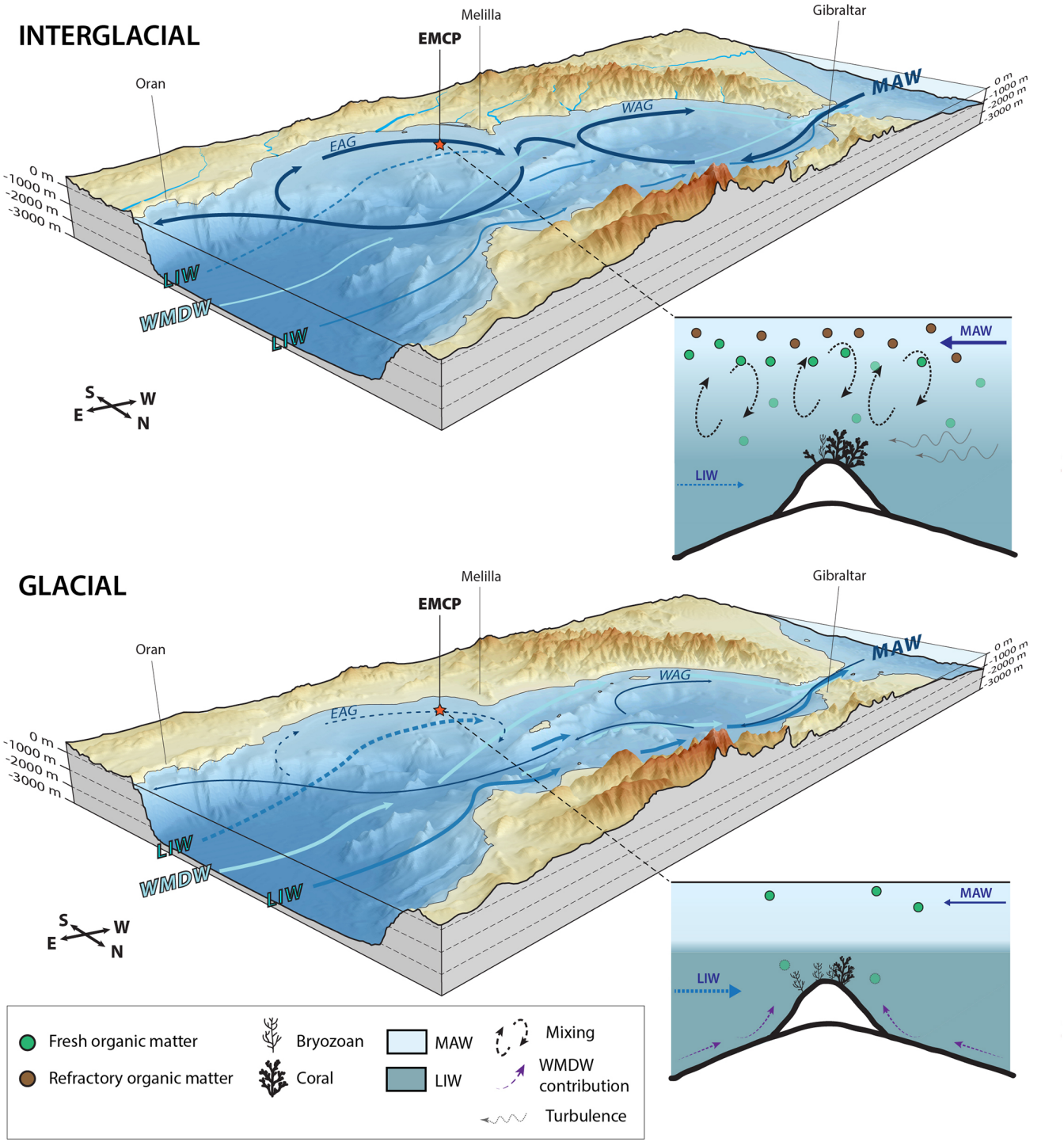

Figure 10. Three-dimensional diagrams and schematic models illustrating the differences between interglacial and glacial periods as well as the response of the benthic community at Brittlestar Ridge I. Water masses discussed in the text are illustrated (MAW: Modified Atlantic Water, LIW: Levantine Intermediate Water, WMDW: Western Mediterranean Deep Water) as are the Western Alboran Gyre (WAG) and Eastern Alboran Gyre (EAG). The flow strength of each water mass is depicted by the thickness of the arrows. The red star indicates the location of the East Melilla Coral Province. The position of the EAG and WAG is based on observations made by Lanoix (1974), La Violette (1983), and Viúdez and Tintoré (1995). Sea level of interglacial periods corresponds to the current sea level, whilst a 100 m lower sea level stand, following observations made by Rabineau et al. (2006), illustrates glacial periods. The LIW and WMDW flows have been simplified and thus do not represent their exact dynamics. The schematic models are not to scale, although relative depth limits between MAW and LIW have been respected. GEBCO_2019 gridded bathymetric data were used to construct the diagrams.

MIS 4, suggest that water mass stratification was greater than during interglacial periods and that the seafloor was not under the direct influence of surface MAW. During glacial periods, the flow of MAW was reduced due to lower sea level and the reduced evaporation over the Mediterranean (Sierro et al., 2005). This would have reduced the contribution of MAW to LIW and weakened the Western and Eastern Alboran Gyres, which would have in turn led to less mixing between surface and intermediate water masses, whilst conversely increasing stratification (Fig. 10). Modern observations show that recently formed dense waters do not necessarily reach the deep western Mediterranean but may, in contrast, be located at intermediate water depths above 1500 m depth (Sparnocchia et al., 1995; Millot, 1999; Ercilla et al., 2016). Ercilla et al. (2016) further revealed that WMDW can be identified at depths shallower than 500 m depth along the Moroccan margin and that it contributes to the overlying LIW, whilst deep-water overturning and ventilation peaked during MIS 2 (Cacho et al., 2006; Toucanne et al., 2012). Increased oxygenation of the seafloor, as evidenced by the benthic foraminiferal assemblage (Fig. 8), may suggest that the contribution of well-ventilated deep and intermediate water masses at BRI was more important during glacials than during interglacials (Fig. 10). The physical shape and structure of BRI possibly plays a role in the shoaling of deep waters during glacial periods. In addition, the overall higher benthic ^{13}C values and the abundance of fresh-organic-matter-feeding foraminifera (*L. lobatula* and *D. coronata*) during glacial periods could indicate that these waters were also nutrient-rich. Although stratification between surface and intermediate water masses was greater during glacials, the stronger flow of well-ventilated WMDW at BRI would explain the higher oxygen availability at the seafloor. Overall during glacial periods, and in particular during the Last Glacial Maximum (LGM), enhanced contribution of nutrition-rich and well-ventilated WMDW to overlying LIW would have promoted mound aggradation.

6 Conclusions

The multiproxy study of core MD13-3462G reveals that mound build-up at the northern part of Brittlestar Ridge I (East Melilla Coral Province, SE Alboran Sea) took place during both interglacial and glacial periods. A number of key observations can be underlined.

1. Average coral mound aggradation rates are particularly low, varying between 1 and 10 cm kyr^{-1}, whilst maximum aggradation rates are recorded during MIS 3 (18 cm kyr^{-1}). These rates suggest that corals never thrived in this sector of Brittlestar Ridge I but rather developed under stressful environmental conditions. We propose that weak bottom-water oxygenation linked to sapropel-related events and/or increased precipitation over North Africa led to the slow development of coral communities during interglacial periods. Intensified circulation of Levantine Intermediate Water and the import of fresh organic matter would have provided suitable conditions for bryozoan and coral communities during glacial periods.

2. Core MD13-3462G provides the first record of consistent coral growth during the last glacial period in the East Melilla Coral Province and more generally in the Alboran Sea. This conspicuous observation, in conjunction with other records of Mediterranean long-term coral mound build-up, suggests that coral mound development does not follow a clear-cut interglacial–glacial pattern in the western Mediterranean. Furthermore, regional- and local-scale environmental variability appears to play a decisive role in mound build-up in the eastern Alboran Sea.

3. The planktonic and benthic $\delta^{18}O$ records of cold-water coral mound sediments at Brittlestar Ridge I show typical interglacial–glacial variations since early MIS 6. This is in contrast with $\delta^{18}O$ records generally recovered from coral mound deposits and highlights that the northern part of Brittlestar Ridge I experienced reduced albeit continuous build-up.

From a wider perspective, the build-up of cold-water coral mounds situated at Brittlestar Ridge I during both interglacial and glacial periods stresses how cold-water coral communities are capable of withstanding important environmental changes as well as surviving and adapting to different climatic conditions. This study further shows that the role of associated species, such as rigid erect bryozoans, may be linked to the resilience of coral ecosystems.

Data availability. The datasets used in this study are available at the open-access repository PANGEA: https://doi.org/10.1594/PANGAEA.915601 (Fentimen et al., 2020c).

Sample availability. Archive halves of all core sections investigated for this study are available at the Department of Geosciences, University of Fribourg (Switzerland). The sediment residues and the splits of each sample analysed for benthic foraminiferal assemblages are stored at the Department of Geosciences, University of Fribourg (Switzerland). Bryozoans identified in this study are available at the Palaeontological Museum of the University of Catania (Italy).

Author contributions. RF was responsible for writing (original draft), visualization, conceptualization, core sampling, and investigation (benthic foraminiferal assemblages, main macrofaunal fragments, particle size analysis, stable isotope measurements assisted by TV, and radiocarbon dating assisted by IH). EF was responsible for conceptualization, writing (review and editing), XRF inves-

tigation (assisted by HV), and preparation of samples for uranium-series dating and Rock-Eval6 pyrolysis. ARü was responsible for conceptualization, writing (review and editing), and supervision. EH was responsible for investigation (CT analysis, macrofaunal quantification). VR was responsible for writing (review and editing) and visualization. TV was responsible for writing (review and editing), investigation (stable isotope measurements), and resources. IH was responsible for writing (review and editing), investigation (radiocarbon dating), and resources. ARo was responsible for writing (review and editing) and investigation (bryozoan taxonomy). DVR was responsible for writing (review and editing) and resources. TA was responsible for writing (review and editing), investigation (Rock-Eval6 pyrolysis), and resources. HV was responsible for writing (review and editing), investigation (XRF), and resources. NF was responsible for writing (review and editing) and investigation (uranium-series dating). AF was responsible for investigation (core description, CT data analysis, XRF data analysis), conceptualization, writing (review and editing), project administration, funding acquisition, and supervision.

Competing interests. The contact author has declared that none of the authors has any competing interests.

Disclaimer. Publisher's note: Copernicus Publications remains neutral with regard to jurisdictional claims in published maps and institutional affiliations.

Acknowledgements. We are grateful for the ship time provided by IPEV on the R/V *Marion Dufresne II* within the framework of the EUROFLEETS GATEWAYS project (grant no. 228344). We further thank Tim Collart for the help he provided with the Rysgran package for R and Marc Schori for his help with the ArcGIS software. We further acknowledge the help of Rene Eichstädter and Andrea Schröder-Ritzrau regarding uranium-series dating and quality control. The DFG has provided funding for the uranium-series dating of corals via the project FR1341/9-1.

Financial support. This research has been supported by the Schweizerischer Nationalfonds zur Förderung der Wissenschaftlichen Forschung (grant nos. 200020_153125 and 200021_149247).

Review statement. This paper was edited by Alessio Rovere and reviewed by two anonymous referees.

References

Addamo, A. M., Vertino, A., Stolarski, J., García-Jiménez, R., Taviani, M., and Machordom, A.: Merging scleractinian genera: the overwhelming genetic similarity between solitary *Desmophyllum* and colonial *Lophelia*, BMC Evol. Biol., 16, 108, https://doi.org/10.1186/s12862-016-0654-8, 2016.

Altenbach, A. V. and Sarnthein, M.: Productivity Record in Benthic Foraminifera, in: Productivity of the Ocean: Present and Past, edited by: Berger, W. H., Smetacek, V. S., and Wefer, G., John Wiley & Sons Limited, Wiley-Interscience, 255–269, 1989.

Angeletti, L., Castellan, G., Montagna, P., Remia, A., and Taviani, M.: The "Corsica Channel Cold-Water Coral Province" (Mediterranean Sea), Front. Mar. Sci., 7, https://doi.org/10.3389/fmars.2020.00661, 2020.

Bahr, A., Kaboth, S., Jiménez-Espejo, F. J., Sierro, F. J., Voelker, A. H. L., Lourens, L., Röhl, U., Reichart, G. J., Escutia, C., Hernández-Molina, F. J., Pross, J., and Friedrich, O.: Persistent monsoonal forcing of mediterranean outflow water dynamics during the late Pleistocene, Geology, 43, 951–954, 2015.

Best, M. A. and Thorpe, J. P.: Particle size, clearance rate and feeding efficiency in marine Bryozoa, in: Biology and Palaeobiology of Bryozoans, edited by: Hayward, P. J., Ryland, J. S., and Taylor, P. D., Olsen and Olsen, Fredensborg, Denmark, 9–14, Olsen and Olsen, 1994.

Beuck, L. and Freiwald, A.: Bioerosion patterns in a deep-water *Lophelia pertusa* (Scleractinia) thicket (Propeller Mound, northern Porcupine Seabight), in: Cold-water corals and ecosystems, edited by: Freiwald, A. and Roberts, J. M., Springer-Verlag, Berlin Heidelberg, 915–936, https://doi.org/10.1007/3-540-27673-4, 2005.

Bjerager, M. and Surlyk, F.: Benthic palaeoecology of Danian deep-shelf bryozoan mounds in the Danish Basin, Palaeogeogr. Palaeocl., 250, 184–215, 2007.

Bout-Roumazeilles, V., Combourieu Nebout, N., Peyron, O., Cortijo, E., Landais, A., and Masson-Delmotte, V.: Connection between South Mediterranean climate and North African atmospheric circulation during the last 50,000 yr BP North Atlantic cold events, Quaternary Sci. Rev., 26, 3197–3215, 2007.

Braun, K., Nehme, C., Pickering, R., Rogerson, M., and Scroxton, N.: A window into Africa's past hydoclimates: the SISAL_V1 database contribution, Quaternary, 2, 4, https://doi.org/10.3390/quat2010004, 2019.

Bromley, R. G.: Preliminary study of bioerosion in the deep-water coral *Lophelia*, Pleistocene, Rhodes, Greece, in: Cold-water Corals and Ecosystems, edited by: Freiwald, A. and Roberts, J. M., Springer-Verlag, Berlin Heidelberg, 895–914, 2005.

Cacho, I., Grimalt, J. O., Pelejero, C., Canals, M., Sierro, F. J., Flores, J. A., and Shackleton, N.: Dansgaard-Oeschger and Heinrich event imprints in Alboran Sea paleotemperatures, Paleoceanography, 14, 698–705, 1999.

Cacho, I., Grimalt, J. O., Sierro, F. J., Scackleton, N. J., and Canals, M.: Evidence for enhanced Mediterranean thermohaline circulation during rapid climatic coolings, Earth Planet Sc. Lett., 183, 417–429, 2000.

Cacho, I., Shackleton, N., Elderfield, H., Sierro, F. J., and Grimalt, J. O.: Glacial rapid variability in deep-water temperature and $\delta^{18}O$ from the Western Mediterranean Sea, Quaternary Sci. Rev., 25, 3294–3311, 2006.

Calvert, S. E. and Pedersen, T. F.: Elemental Proxies for Palaeoclimatic and Palaeoceanographic Variability in Marine Sediments: Interpretation and Application, in: Developments in Marine Geology, edited by: Hillaire-Marcel, C. and De Vernal, A., Elsevier, ISBN 978-0-444-52755-4, https://doi.org/10.1016/S1572-5480(07)01019-6, 2007.

Camafort, M., Gracia, E., and Ranero, C. R.: Quaternary Seismostratigraphy and Tectonosedimentary Evolution of the North Tunisian Continental Margin, Tectonics, 39, e2020TC006243, https://doi.org/10.1029/2020TC0062432020,

Caquineau, S., Gaudichet, A., Gomes, L., Magonthier, M.-C., and Chatenet, B.: Saharan dust: Clay ratio as a relevant tracer to assess the origin of soil-derived aerosols, Geophys. Res. Lett., 25, 983–986, 1998.

Caquineau, S., Gaudichet, A., Gomes, L., and Legrand, M.: Mineralogy of Saharan dust transported over northwestern tropical Atlantic Ocean in relation to source regions, J. Geophys. Res.-Atmos., 107, 1–14, 2002.

Carlier, A., Le Guilloux, E., Olu, K., Sarrazin, J., Mastrototaro, F., Taviani, M., and Clavier, J.: Trophic relationships in a deep Mediterranean cold-water coral bank (Santa Maria di Leuca, Ionian Sea), Mar. Ecol. Prog. Ser., 397, 125–137, 2009.

Cheng, H., Adkins, J., Lawrence Edwards, R., and Boyle, E. A.: U-Th dating of deep-sea corals, Geochim. Cosmochim. Ac., 64, 2401–2416, https://doi.org/10.1016/S0016-7037(99)00422-6, 2000.

Clarke, K. R. and Gorley, R. N.: PRIMER v6: User Manual/Tutorial (Plymouth Routines in Multivariate Ecological Research), PRIMER-E, Plymouth, 190 pp., 2006.

Cleveland, W. S. and Devlin, S. J.: Regression Analysis by Local Fitting, J. Am. Stat. Assoc., 83, 596–610, 1986.

Comas, M. and Pinheiro, L. M.: The Melilla carbonate mounds: do deep-water coral mounds count on seeping fluids in the Alboran Sea?, Rapp. Comm. Int. Mer Médit, 39, p. 16, 2010.

Comas, M. C., Platt, J. P., Soto, J. I., and Watts, A. B.: The origin and tectonic history of the Alboran Basin: insights from Leg 161 results, Proceedings of the Ocean Drilling Program 161, Sci. Results, 555–580, 1999.

Comas, M. C., Pinheiro, L. M., Ivanov, M., and TTR-17 Leg 1 Scientific Party: Deep-water coral mounds in the Alboran Sea: the Melilla mounds field revisited, IOC Workshop Report No. 220, Granada (Spain), Workshop report, 2–5 February 2009, 2009.

Corbera, G., Lo Iacono, C., Gràcia, E., Grinyo, J., Pierdomenico, M., Huvenne, V. A. I., Aguilar, R., and Gili, J. M.: Ecological characterisation of a Mediterranean cold-water coral reef: Cabliers Coral Mound Province (Alboran Sea, western Mediterranean), Prog. Oceanogr., 175, 245–262, 2019.

Corbera, G., Lo Iacono, C., Standish, D., Anagnostou, E., Titschack, J., Katsamenis, O., Cacho, I., Van Rooij, D., Huvenne, V. A. I., and Foster, G. L.: Glacio-eustatic variations and sapropel events as main controls on the Middle Pleistocene-Holocene evolution of the Cabliers Coral Mound Province (W Mediterranean), Quaternary Sci. Rev., 253, 106783, https://doi.org/10.1016/j.quascirev.2020.106783, 2021.

Corbera, G., Lo Iacono, C., Standish, C. D., Gràcia, E., Ranero, C., Huvenne, V. A. I., Anagnostou, E., and Foster, G. L.: Glacial-aged development of the Tunisian Coral Mound Province controlled by glacio-eustatic oscillations and changes in surface productivity, Mar. Geol., 446, 106772, https://doi.org/10.1016/j.margeo.2022.106772, 2022.

Coulthard, T. J., Ramirez, J. A., Barton, N., Rogerson, M., and Brucher, T.: Were rivers flowing across the Sahara during the last interglacial? Implications for human migration through Africa, PLoS One, 8, e74834, https://doi.org/10.1371/journal.pone.0074834, 2013.

Davies, A. J. and Guinotte, J. M.: Global habitat suitability for framework-forming cold-water corals, PLoS One, 6, e18483, https://doi.org/10.1371/journal.pone.0018483, 2011.

Davies, A. J., Duineveld, G., Lavaleye, M., Bergman, M., van Haren, H., and Roberts, J.: Downwelling and deep-water bottom currents as food supply mechanisms to the cold-water coral *Lophelia pertusa* (*Scleractinia*) at the Mingulay Reef Complex, Limnol. Oceanogr., 54, 620–629, 2009.

De Mol, B., Van Rensbergen, P., Pillen, S., Van Herreweghe, K., Van Rooij, D., McDonnell, A., Huvenne, V. A. I., Ivanov, M., Swennen, R., and Henriet, J.-P.: Large deep-water coral banks in the Porcupine Basin, southwest of Ireland, Mar. Geol., 188, 193–231, 2002.

De Rijk, S., Jorissen, F., Rohling, E. J., and Troelstra, S. R.: Organic flux control on bathymetric zonation of Mediterranean benthic foraminifera, Mar. Micropaleontol., 40, 151–166, 2000.

Dessandier, P.-A., Bonnin, J., Kim, J.-H., Bichon, S., Deflandre, B., Grémare, A., and Sinninghe Damsté, J. S.: Impact of organic matter source and quality on living benthic foraminiferal distribution on a river-dominated continental margin: A study of the Portuguese margin, J. Geophys. Res.-Biogeo., 121, 1689–1714, 2016.

Dorschel, B., Hebbeln, D., Ruggeberg, A., Dullo, W.-C., and Freiwald, A.: Growth and erosion of a cold-water coral covered carbonate mound in the Northeast Atlantic during the Late Pleistocene and Holocene, Earth Planet Sc. Lett., 233, 33–44, 2005.

Dorschel, B., Hebbeln, D., Foubert, A., White, M., and Wheeler, A.J.: Hydrodynamics and cold-water coral facies distribution related to recent sedimentary processes at Galway Mound west of Ireland, Mar. Geol., 244, 184–195, 2007.

Drinia, H. and Dermitzakis, M. D.: The response of benthic foraminifera to palaeoenvironmental disturbance: A quantitative approach in turbidite-like successions, N. Jb. Geol. Paläont. Abh, 258, 325–338, 2010.

Duggen, S., Hoernle, K., Klügel, A., Geldmacher, J., Thirlwall, M., Hauff, F., Lowry, D., and Oates, N.: Geochemical zonation of the Miocene Alborán Basin volcanism (westernmost Mediterranean): geodynamic implications, Contrib. Mineral. Petr., 156, 577–593, 2008.

Dullo, W.-C., Flögel, S., and Rüggeberg, A.: Cold-water coral growth in relation to the hydrography of the Celtic and Nordic European continental margin, Mar. Ecol. Prog. Ser., 371, 165–176, 2008.

Eisele, M., Hebbeln, D., and Wienberg, C.: Growth history of a cold-water coral covered carbonate mound – Galway Mound, Porcupine Seabight, NE-Atlantic, Mar. Geol., 253, 160–169, 2008.

Eisele, M., Frank, N., Wienberg, C., Hebbeln, D., López Correa, M., Douville, E., and Freiwald, A.: Productivity controlled cold-water coral growth periods during the last glacial off Mauritania, Mar. Geol., 280, 143–149, 2011.

Emelyanov, E. M. and Shimkus, K. M.: Geochemistry and sedimentology of the Mediterranean Sea, Springer Science and Business Media, Springer Dordrecht, https://doi.org/10.1007/978-94-009-4490-9, 2012.

Emig, C. C. and Arnaud, P. M.: Observations en submersible sur la densité des populations de *Gryphus vitreus* (Brachiopode) le long de la marge continentale de Provence (Méditerranée nord-occidentale), C. R. Acad. Sci. Paris, 306, 501–505, 1988.

Ercilla, G., Juan, C., Hernández-Molina, J., Bruno, M., Estrada, F., Alonso, B., Casas, D., Farran, M., Llave, E., García, Vázquez, J.T., D'Acremont, E., Gorini, C., Palomino, D., Valencia, J., El Moumni, B., and Ammar, A.: Significance of bottom currents in deep-sea morphodynamics: An example from the Alboran Sea, Mar. Geol., 378, 157–170, 2016.

Espitalié, J., Deroo, G., and Marquis, F.: La Pyrolyse Rock-Eval et ses applications, Revue de l'Institut Français du Pétrole, 40, 1–34, 1985.

Fantasia, A., Adatte, T., Spangenberg, J. E., Font, E., Duarte, L. V., and Föllmi, K. B.: Global versus local processes during the Pliensbachian-Toarcian transition at the Peniche GSSP, Portugal: a multi-proxy record, Earth-Sci. Rev., 198, 102932, https://doi.org/10.1016/j.earscirev.2019.102932, 2019.

Fariduddin, M. and Loubere, P.: The surface ocean productivity response of deeper water benthic foraminifera in the Atlantic Ocean, Mar. Micropaleontol., 32, 289–310, 1997.

Fentimen, R., Feenstra, E., Rüggeberg, A., Vennemann, T., Hajdas, I., Adatte, T., Van Rooij, D., and Foubert, A.: Cold-Water Coral Mound Archive Provides Unique Insights Into Intermediate Water Mass Dynamics in the Alboran Sea During the Last Deglaciation, Front. Mar. Sci., 7, 354, https://doi.org/10.3389/fmars.2020.00354, 2020a.

Fentimen, R., Lim, A., Rüggeberg, A., Wheeler, A. J., Van Rooij, D., and Foubert, A.: Impact of bottom water currents on benthic foraminiferal assemblages in a cold-water coral environment: The Moira Mounds (NE Atlantic), Mar. Micropaleontol, 154, 101799, https://doi.org/10.1016/j.marmicro.2019.101799, 2020b.

Fentimen, R., Feenstra, E., Rüggeberg, A., Hall, E., Rime, V., Vennemann, T. W., Hajdas, I., Rosso, A., Van Rooij, D., Adatte, T., Vogel, H., Frank, N., Krengel, T., and Foubert, A.: Geochemistry, benthic foraminifera and grain size distribution in sediment core MD13-3462G, PANGAEA [data set], https://doi.pangaea.de/10.1594/PANGAEA.915601, 2020c.

Filippidi, A., Triantaphyllou, M. V., and De Lange, G. J.: Eastern-Mediterranean ventilation variability during sapropel S1 formation, evaluated at two sites influenced by deep-water formation from Adriatic and Aegean Seas, Quaternary Sci. Rev., 144, 95–106, 2016.

Fink, H. G., Wienberg, C., De Pol-Holz, R., Wintersteller, P., and Hebbeln, D.: Cold-water coral growth in the Alboran Sea related to high productivity during the Late Pleistocene and Holocene, Mar. Geol., 339, 71–82, 2013.

Fink, H. G., Wienberg, C., De Pol-Holz, R., and Hebbeln, D.: Spatio-temporal distribution patterns of Mediterranean cold-water corals (*Lophelia pertusa* and *Madrepora oculata*) during the past 14,000 years, Deep-Sea Res. Pt. I, 103, 37–48, 2015.

Folk, R. L. and Ward, W. C.: A Study in the Significance of Grain-Size Parameters, J. Sediment. Petrol., 27, 3–26, 1957.

Fontanier, C., Jorissen, F. J., Licari, L., Alexandre, A., Anschutz, P., and Carbonel, P.: Live benthic foraminiferal faunas from the Bay of Biscay: faunal density, composition, and microhabitats, Deep-Sea Res. Pt. I, 49, 751–785, 2002.

Fontanier, C., Jorissen, F. J., Chaillou, G., David, C., Anschutz, P., and Lafon, V.: Seasonal and interannual variability of benthic foraminiferal faunas at 550 m depth in the Bay of Biscay, Deep-Sea Res. Pt. I, 50, 457–494, 2003.

Foubert, A. and Henriet, J.-P.: Nature and Significance of the Recent Carbonate Mound Record, Lecture Notes in Earth Sciences, 126, Springer-Verlag, Berlin, 298 pp., https://doi.org/10.1007/978-3-642-00290-8, 2009.

Frank, N., Paterne, M., Ayliffe, L., van Weering, T., Henriet, J.-P., and Blamart, D.: Eastern North Atlantic deep-sea corals: tracing upper intermediate water $\Delta^{14}C$ during the Holocene, Earth Planet Sc. Lett., 219, 297–309, 2004.

Frank, N., Ricard, E., Lutringer-Paquet, A., van der Land, C., Colin, C., Blamart, D., Foubert, A., Van Rooij, D., Henriet, J.-P., de Haas, H., and van Weering, T.: The Holocene occurrence of cold water corals in the NE Atlantic: Implications for coral carbonate mound evolution, Mar. Geol., 266, 129–142, 2009.

Frank, N., Freiwald, A., Correa, M. L., Wienberg, C., Eisele, M., Hebbeln, D., Van Rooij, D., Henriet, J. P., Colin, C., van Weering, T., de Haas, H., Buhl-Mortensen, P., Roberts, J. M., De Mol, B., Douville, E., Blamart, D., and Hatte, C.: Northeastern Atlantic cold-water coral reefs and climate, Geology, 39, 743–746, 2011.

Freiwald, A., Fosså, J. H., Grehan, A., Koslow, T., and Roberts, J. M.: Cold-water coral Reefs, UNEP_WCMC, Cambridge, UK, UNEP-WCMC, ISBN 9789280724530, 2004.

Freiwald, A., Beuck, L., Rüggeberg, A., Taviani, M., and Hebbeln, D: The white coral community in the central Mediterranean Sea revealed by ROV surveys, Oceanography, 22, 58–74, 2009.

Gasse, F.: Hydrological changes in the African tropics since the Last Glacial Maximum, Quaternary Sci. Rev., 19, 189–211, 2000.

Gasse, F. and Roberts, C. N.: Late Quaternary hydrologic changes in the arid and semiarid belt of northern Africa, in: The Hadley Circulation: Present, Past and Future, edited by: Diaz, H. F. and Bradley, R. S., Kluwer Academic Publishers, Springer Dordrecht, 313–345, https://doi.org/10.1007/978-1-4020-2944-8, 2005.

Gilbert, E. R., Camargo, M. G. and Sandrini-Neto, L.: rysgran: Grain size analysis, textural classifications and distribution of unconsolidated sediments, R package version 2.1.0, https://CRAN.R-project.org/package=rysgran (last access: 1 May 2019), 2015.

Goldstein, S. T.: Foraminifera: A biological overview, in: Modern Foraminifera, edited by: Sen Gupta, B. K., 37–55, Kluwer Acad., Norwell, Mass., Springer Dordrecht, https://doi.org/10.1007/0-306-48104-9, 1999.

Gooday, A. J.: The Biology of Deep-Sea Foraminifera: A Review of Some Advances and Their Applications in Paleoceanography, Palaios, 9, 14–31, 1993.

Gregory, B. R. B., Patterson, T. R., Reinhardt, E. G., Galloway, J. M., and Roe, H. R.: An evaluation of methodologies for calibrating Itrax X-ray fluorescence counts with ICP-MS concentration data for discrete sediment samples, Chem. Geol., 525, 12–27, 2019.

Guieu, C. and Thomas, A. J.: Saharan Aerosols: From the Soil to the Ocean, in: The Impact of Desert Dust Across the Mediterranean, edited by: Guerzoni, S. and Chester, R., Springer Netherlands, Dordrecht, 408 pp., https://doi.org/10.1007/978-94-017-3354-0, 1996.

Hanz, U., Wienberg, C., Hebbeln, D., Duineveld, G., Lavaleye, M., Juva, K., Dullo, W.-C., Freiwald, A., Tamborrino, L., Reichart, G.-J., Flögel, S., and Mienis, F.: Environmental factors influencing benthic communities in the oxygen minimum zones on the Angolan and Namibian margins, Biogeosciences, 16, 4337–4356, https://doi.org/10.5194/bg-16-4337-2019, 2019.

Hebbeln, D.: Highly variable submarine landscapes in the Alborán Sea created by cold-water corals, in: Mediterranean Cold-Water Corals: Past, Present and Future, edited by: Orejas, C. and Jiménez, C., Springer series: Coral Reefs of the World 9, Springer International Publishing, 61–65, Springer, Cham, https://doi.org/10.1007/978-3-319-91608-8_8, 2019.

Hebbeln, D., Van Rooij, D., and Wienberg, C.: Good neighbours shaped by vigorous currents: Cold-water coral mounds and contourites in the North Atlantic, Mar. Geol., 378, 171–185, 2016.

Heburn, G. W. and La Violette, P. E.: Variations in the structure of the anticyclonic gyres found in the Alboran Sea, J. Geophys. Res., 95, 1599–1613, https://doi.org/10.1029/JC095iC02p01599, 1990.

Holbourn, A., Kuhnt, W., and, James, N.: Late Pleistocene bryozoan reef mounds of the Great Australian Bight: Isotope stratigraphy and benthic foraminiferal record, Paleoceanography, 17, https://doi.org/10.1029/2001PA000643, 2002.

Huvenne, V. A. I., De Haas, H., Dekindt, K., Henriet, J-P., Kozachenko, M., Olu-Le Roy, K., and Wheeler, A. J.: The seabed appearance of different coral bank provinces in the Porcupine Seabight, NE Atlantic: results from sidescan sonar and ROV seabed mapping, in: Cold-water Corals and Ecosystems, edited by: Freiwald, A. and Roberts, J. M., Springer-Verlag, Berlin, Heidelberg, 536–569, https://doi.org/10.1007/3-540-27673-4, 2005.

Huvenne, V. A. I., Masson, D. G., and Wheeler, A. J.: Sediment dynamics of a sandy contourite: the sedimentary context of the Darwin cold-water coral mounds, Northern Rockall Trough, Int. J. Earth Sci.,98, 865–884, 2009.

Jaffey, A. H., Flynn, K. F., Glendenin, L. E., Bentley, W. C., and Essling, A. M.: Precision measurements of half-lives and specific activities of ^{235}U and ^{238}U, Phys. Rev., 4, 5, 1889–1906, 1971.

James, N. P., Feary, D. A., Surlyk, F., Toni Simo, J. A., Betzler, C., Holbourn, A. E., Li, Q., Matsuda, H., Machiyama, H., Brooks, G. R., Andres, M. S., Hine, A. C., and Malone, M. J.: Quaternary bryozoan reef mounds in cool-water, upper slope environments: Great Australian Bight, Geology, 28, 647–650, https://doi.org/10.1130/0091-7613(2000)28<647:Qbrmic>2.0.Co;2, 2000.

Jorissen, F. J.: The distribution of benthic foraminifera in the Adriatic Sea, Mar. Micropaleontol., 12, 21–48, 1987.

Jorissen, F. J.: Benthic foraminiferal successions across Late Quaternary Mediterranean sapropels, Mar. Geol., 153, 91–101, 1999.

Kano, A., Ferdelman, T. G., Williams, T., Henriet, J.-P., Ishikawa, T., Kawagoe, N., Takashima, C., Kakizaki, Y., Abe, K., Sakai, S., Browning, E. L., and Li, X.: Age constraints on the origin and growth history of a deep-water coral mound in the northeast Atlantic drilled during Integrated Ocean Drilling Program Expedition 307, Geology, 35, 1051–1054, https://doi.org/10.1130/G23917A.1, 2007.

Katz, E. J.: The Levantine Intermediate Water between the Strait of Sicily and the Strait of Gibraltar, Deep-Sea Res., 19, 507–520, 1972.

Kenyon, N. H., Akhmetzhanov, A. M., Wheeler, A. J., van Weering, T. C. E., de Haas, H., and Ivanov, M. K.: Giant carbonate mud mounds in the southern Rockall Trough, Mar. Geol., 195, 5–30, 2003.

Knippertz, P., Christoph, M., and Speth, P.: Long-term precipitation variability in Morocco and the link to the large-scale circulation in recent and future climates, Meteorol. Atmos. Phys., 83, 67–88, 2003.

Koho, K. A., García, R., de Stigter, H. C., Epping, E., Koning, E., Kouwenhoven, T. J., and van der Zwaan, G. J.: Sedimentary labile organic carbon and pore water redox control on species distribution of benthic foraminifera: A case study from Lisbon–Setúbal Canyon (southern Portugal), Prog. Oceanogr., 79, 55–82, 2008.

Krengel, T.: 550,000 years of marine climate variability in the western Mediterranean Sea revealed by cold-water corals, PhD thesis, Heidelberg University (Germany), 189 pp., Universität Bibliotek Heidelberg, https://doi.org/10.11588/heidok.00027990, 2020.

Lavaysse, C., Flamant, C., Janicot, S., Parker, D. J., Lafore, J.-P., Sultan, B., and Pelon, J.: Seasonal evolution of the West African heat low: a climatological perspective, Clim. Dynam,, 33, 313–330, 2009.

La Violette, P. E.: The Advection of Submesoscale Thermal Features in the Alboran Sea Gyres, J. Phys. Oceanogr., 14, 550–565, 1983.

Lafuente, J. G., Camno, N., Vargas, M., Rubín, J. P., and Hernández-Guerra, A.: Evolution of the Alboran Sea hydrographic structures during July 1993, Deep-Sea Res. Pt. I, 45, 39–65, 1998.

Lanoix, R.: Projet Alboran: étude hydrologique et dynamique de la mer d'Alboran, Technical Report 66, NATO, Brussels, Belgium, impr. SIRCO France, 1974.

Linke, P. and Lutze, G. F.: Microhabitat preferences of benthic foraminifera – a static concept or a dynamic adaptation to optimize food acquisition?, Mar. Micropaleontol., 20, 215–234, 1993.

Lionello, P., Trigo, I. F., Gil, V., Liberato, M. L. R., Nissen, K. M., Pinto, J. G., Raible, C. C., Reale, M., Tanzarella, A., Trigo, R. M., Ulbrich, S., and Ulbrich U.: Objective climatology of cyclones in the Mediterranean region: a consensus view among methods with different system identification and tracking criteria, Tellus A, 68, 29391, https://doi.org/10.3402/tellusa.v68.29391, 2016.

Lisiecki, L. E. and Raymo, M. E.: A Pliocene-Pleistocene stack of 57 globally distributed benthic δ^{18}O records, Paleoceanography, 20, PA1003, https://doi.org/10.1029/2004PA001071, 2005.

Lo Iacono, C., Gràcia, E., Ranero, C. R., Emelianov, M., Huvenne, V. A. I., Bartolomé, R., Booth-Rea, G., Prades, J., Ambroso, S., Dominguez, C., Grinyó, J., Rubio, E., and Torrent, J.: The West Melilla cold water coral mounds, Eastern Alboran Sea: Morphological characterization and environmental context, Deep-Sea Res. Pt. II, 99, 316–326, 2014.

López Correa, M., Montagna, P., Joseph, N., Rüggeberg, A., Fietzke, J., Flögel, S., Dorschel, B., Goldstein, S. L., Wheeler, A., and Freiwald, A.: Preboreal onset of cold-water coral growth beyond the Arctic Circle revealed by coupled radiocarbon and U-series dating and neodymium isotopes, Quaternary Sci. Rev., 34, 24–43, 2012.

Löwemark, L., Chen, H. F., Yang, T. N., Kylander, M., Yu, E. F., Hsu, Y. W., Lee, T. Q., Song, S. R., and Jarvis, S.: Normalizing XRF-scanner data: A cautionary note on the interpretation of high-resolution records from organic-rich lakes, J. Asian Earth Sci., 40, 1250–56, 2011.

Lutze, G. F. and Coulbourn, W. T.: Recent benthic foraminifera from the continental margin of Northwest Africa: community structure and distribution, Mar. Micropaleontol., 8, 361–401, 1984.

Mackensen, A., Schmiedl, G., Harloff, J., and Giese, M.: Deep-sea foraminifera in the South Atlantic Ocean: Ecology and assemblage generation, Micropaleontology, 41, 342–358, 1995.

Margreth, S., Rüggeberg, A., and Spezzaferri, S.: Benthic foraminifera as bioindicator for cold-water coral reef ecosystems along the Irish margin, Deep-Sea Res. Pt. I, 56, 2216–2234, 2009.

Martinez-Ruiz, F., Kastner, M., Gallego-Torres, D., Rodrigo-Gámiz, M., Nieto-Moreno, V., and Ortega-Huertas, M.: Paleoclimate and paleoceanography over the past 20,000 yr in the Mediterranean Sea Basins as indicated by sediment elemental proxies, Quaternary Sci. Rev., 107, 25–46, 2015.

Martins, V., Jouanneau, J.-M., Weber, O., and Rocha, F.: Tracing the late Holocene evolution of the NW Iberian upwelling system, Mar. Micropaleontol., 59, 35–55, 2006.

Martorelli, E., Petroni, G., Chiocci, F. L., and the Pantelleria Scientific Party: Contourites offshore Pantelleria Island (Sicily Channel, Mediterranean Sea): depositional, erosional and biogenic elements, Geo.-Mar. Lett., 31, 481–493, 2011

Martrat, B., Grimalt, J. O., Lopez-Martinez, C., Cacho, I., Sierro, F. J., Flores, J. A., Zahn, R., Canals, M., Curtis, J. H., and Hodell, D. A.: Abrupt temperature changes in the Western Mediterranean over the past 250,000 years, Science, 306, 1762–1765, 2004.

Masqué, P., Fabres, J., Canals, M., Sanchez-Cabeza, J. A., Sanchez-Vidal, A., Cacho, I., Calafat, A. M., and Bruach, J. M: Accumulation rates of major constituents of hemipelagic sediments in the deep Alboran Sea: a centennial perspective of sedimentary dynamics, Mar. Geol., 193, 207–233, 2003.

Mastrototaro, F., D'Onghia, G., Corriero, G., Matarrese, A., Maiorano, P., Panetta, P., Gherardi, M., Longo, C., Rosso, A., Sciuto, F., Sanfilippo, R., Gravili, C., Boero, F, Taviani, M., and Tursi, A.: Biodiversity of the white coral bank off Cape Santa Maria di Leuca (Mediterranean Sea): An update, Deep-Sea Res. Pt. II, 57, 412–430, https://doi.org/10.1016/j.dsr2.2009.08.021, 2010.

Matos, L., Mienis, F., Wienberg, C., Frank, N., Kwiatkowski, C., Groeneveld, J., Thil, F., Abrantes, F., Cunha, M. R., and Hebbeln, D.: Interglacial occurrence of cold-water corals off the Cape Lookout (NW Atlantic): First evidence of the Gulf Stream influence, Deep-Sea Res. Pt. I, 105, 158–170, 2015.

Matos, L., Wienberg, C., Titschack, J., Schmiedl, G., Frank, N., Abrantes, F., Cunha, M. R., and Hebbeln, D.: Coral mound development at the Campeche cold-water coral province, southern Gulf of Mexico: Implications of Antarctic Intermediate Water increased influence during interglacials, Mar. Geol., 392, 53–65, 2017.

McCave, I. N. and Hall, I. R.: Size sorting in marine muds: Processes, pitfalls, and prospects for paleoflow-speed proxies, Geochem. Geophy. Geosy., 7, Q10N05, https://doi.org/10.1029/2006GC001284, 2006.

McCave, I. N., Manighetti, B., and Robinson, S. G.: Sortable silt and fine sediment size/composition slicing: Parameters for palaeocurrent speed and palaeoceanography, Paleoceanography, 10, 593–610, 1995.

Mienis, F., de Stigter, H.C., White, M., Duineveld, G., de Haas, H., and van Weering, T. C. E.: Hydrodynamic controls on cold-water coral growth and carbonate-mound development at the SW and SE Rockall Trough Margin, NE Atlantic Ocean, Deep-Sea Res. Pt. I, 54, 1655–1674, 2007.

Mienis, F., van der Land, C., de Stigter, H. C., van de Vorstenbosch, M., de Haas, H., Richter, T., and van Weering, T. C. E.: Sediment accumulation on a cold-water carbonate mound at the Southwest Rockall Trough margin, Mar. Geol., 265, 40–50, 2009.

Milker, Y., Schmiedl, G., Betzler, C., Römer, M., Jaramillo-Vogel, D., and Siccha, M.: Distribution of recent benthic foraminifera in shelf carbonate environments of the Western Mediterranean Sea, Mar. Micropaleontol., 73, 207–225, 2009.

Millot, C.: Circulation in the western Mediterranean Sea, J. Mar. Syst., 20, 423–442, 1999.

Millot, C.: Another description of the Mediterranean Sea outflow, Prog. Oceanogr., 82, 101–124, 2009.

Millot, C.: Levantine Intermediate Water characteristics: an astounding general misunderstanding!, Sci. Mar., 77, 217–232, 2013.

Millot, C. and Taupier-Letage, I.: Circulation in the Mediterranean Sea, in: The Handbook of Environmental Chemistry: The Mediterranean Sea (HEC5, volume 5k), edited by: Saliot, A., Springer-Verlag Berlin Heidelberg, 29–66, https://doi.org/10.1007/b107143, 2005.

Millot, C., Candela, J., Fuda, J.-L., and Tber, Y.: Large warming and salinification of the Mediterranean outflow due to changes in its composition, Deep-Sea Res. Pt. I, 53, 656–666, 2006.

Mohn, C., Rengstorf, A., White, M., Duineveld, G., Mienis, F., Soetaert, K., and Grehan, A.: Linking benthic hydrodynamics and cold-water coral occurrences: A high-resolution model study at three cold-water coral provinces in the NE Atlantic, Prog. Oceanogr., 122, 92–104, 2014.

Mojtahid, M., Jorissen, F., Lansard, B., Fontanier, C., Bombled, B., and Rabouille, C.: Spatial distribution of live benthic foraminifera in the Rhône prodelta: Faunal response to a continental–marine organic matter gradient, Mar. Micropaleontol., 70, 177–200, 2009.

Murray, J. W.: Ecology and Applications of Benthic Foraminifera, Cambridge University Press, 426 pp., https://doi.org/10.1017/CBO9780511535529, 2006.

Negri, M. P. and Corselli, C.: Bathyal *Mollusca* from the cold-water coral biotope of Santa Maria di Leuca (Apulian margin, southern Italy), Zootaxa, 4186, https://doi.org/10.11646/zootaxa.4186.1.1, 2016.

Olivet, J. L., Auzende, J. M., and Bonnin, J.: Structure et évolution tectonique du bassin d'Alboran, B. Soc. Geol. Fr., 7, 491–495, 1973.

Osborne, A. H., Vance, D., Rohling, E. J., Barton, N., Rogerson, M., and Fello, N.: A humid corridor across the Sahara for the migration of early modern humans out of Africa 120,000 years ago, P. Natl. Acad. Sci. USA, 105, 16444–16447, 2008.

Paillard, D., Labeyrie, L., and Yiou, P.: Macintosh Program performs time Series Analysis, EOS Trans. AGU, 77, https://agupubs.onlinelibrary.wiley.com/doi/abs/10.1029/96EO00259 (last access: 17 August 2022), 1996.

Pasquier, V., Toucanne, S., Sansjofre, P., Dixit, Y., Revillon, S., Mokeddem, Z., and Rabineau, M.: Organic matter isotopes reveal enhanced rainfall activity in Northwestern Mediterranean borderland during warm substages of the last 200 ky, Quaternary Sci. Rev., 205, 182–192, 2018

Pérez-Folgado, M., Sierro, F. J., Flores, J. A., Grimalt, J. O., and Zahn, R.: Paleoclimatic variations in foraminifer assemblages

from the Alboran Sea (Western Mediterranean) during the last 150 ka in ODP Site 977, Mar. Geol., 212, 113–131, 2004.

Phleger, F. B. and Soutar, A.: Production of Benthic Foraminifera in Three East Pacific Oxygen Minima, Micropaleontology, 19, 110–115, 1973.

Pomar, L., Morsilli, M., Hallock, P., and Bádenas, B.: Internal waves, and under-explored source of turbulence events in the sedimentary record, Earth Sci. Rev., 111, 56–81, 2012.

R Core Team: R: A language and environment for statistical computing, R Foundation for Statistical Computing, Vienna, Austria, https://www.R-project.org/ (last access: 17 August 2022), 2018

Rabineau, M., Berné, S., Olivet, J.-L., Aslanian, D., Guillocheau, F., and Joseph, P.: Paleo sea levels reconsidered from direct observation of paleoshoreline position during Glacial Maxima (for the last 500,000 yr), Earth Planet Sc. Lett., 252, 119–137, 2006.

Rachid, J., Hssaida, T., Hamoumi, N., Terhzaz, L., Spezzaferri, S., Frank, N., and Daghor, L.: Palynological study of carbonated mounds during the Holocene along the Atlantic and Mediterranean Moroccan margins, Rev. Palaeobot. Palyno., 278, 104213, https://doi.org/10.1016/j.revpalbo.2020.104213, 2020

Raddatz, J., Rüggeberg, A., Flögel, S., Hathorne, E. C., Liebetrau, V., Eisenhauer, A., and Dullo, W.-Chr.: The influence of seawater pH on U / Ca ratios in the scleractinian cold-water coral Lophelia pertusa, Biogeosciences, 11, 1863–1871, https://doi.org/10.5194/bg-11-1863-2014, 2014.

Ramsey, C.: OxCal 4.2.4, Electronic document, https://c14.arch.ox.ac.uk/oxcal.html (last access: 17 August 2022), 2017.

Reimer, P. J., Bard, E., Bayliss, A., Beck, J. W., Blackwell, P. G., Ramsey, C. B., Buck, C. E., Cheng, H., Edwards, R. L., Friedrich, M., Grootes, P. M., Guilderson, T. P., Haflidason, H., Hajdas, I., Hatté, C., Heaton, T. J., Hoffmann, D. L., Hogg, A. G., Hughen, K. A., Kaiser, K. F., Kromer, B., Manning, S. W., Niu, M., Reimer, R. W., Richards, D. A., Scott, E. M., Southon, J. R., Staff, R. A., Turney, C. S. M., and van der Plicht, J.: IntCal13 and Marine13 Radiocarbon Age Calibration Curves 0–50,000 Years cal BP, Radiocarbon, 55, 1869–1887, 2013.

Remia, A.: Taviani, Shallow-buried Pleistocene Madrepora-dominated coral mounds on a muddy continental slope, Tuscan Archipelago, NE Tyrrhenian Sea, Facies, 50, 419–425, 2005.

Roberts, J. M., Wheeler, A. J., and Freiwald, A.: Reefs of the Deep: The Biology and Geology of Cold-Water Coral Ecosystems, Science, 312, 543–547, 2006.

Roberts, J. M., Wheeler, A. J., Freiwald, A., and Cairns, S.: Cold-Water Corals, Cambridge University Press, 351 pp., https://doi.org/10.1017/CBO9780511581588, 2009.

Rodrigo-Gámiz, M., Martínez-Ruiz, F., Jiménez-Espejo, F. J., Gallego-Torres, D., Nieto-Moreno, V., Romero, O., and Ariztegui, D.: Impact of climate variability in the western Mediterranean during the last 20,000 years: oceanic and atmospheric responses, Quaternary Sci. Rev., 30, 2018–2034, 2011.

Rohling, E. J., Cane, T. R., Cooke, S., Sprovieri, M., Bouloubassi, I., Emeis, K. C., Schiebel, R., Kroon, D., Jorissen, F. J., Lorre, A., and Kemp, A. E. S.: African monsoon variability during the previous interglacial maximum, Earth Planet Sc. Lett., 202, 61–75, 2002.

Rüggeberg, A., Dullo, C., Dorschel, B., and Hebbeln, D.: Environmental changes and growth history of a cold-water carbonate mound (Propeller Mound, Porcupine Seabight), Int. J. Earth Sci., 96, 57–72, 2007.

Sánchez-Guillamón, O., Rueda, J. L., Wienberg, C., Ercilla, G., Vázquez, J. T., Gómez-Ballesteros, M., Urra, J., Moya-Urbano, E., Estrada, F., and Hebbeln, D.: Morphosedimentary, Structural and Benthic Characterization of Carbonate Mound Fields on the Upper Continental Slope of the Northern Alboran Sea (Western Mediterranean), Geosciences, 12, 111, https://doi.org/10.3390/geosciences12030111, 2022.

Schiebel, R. and Hemleben, C.: Planktic Foraminifers in the Modern Ocean, Springer-Verlag, Berlin, Heidelberg, 358 pp., https://doi.org/10.1007/978-3-662-50297-6, 2017.

Schmiedl, G. and Mackensen, A.: Late Quaternary paleoproductivity and deep water circulation in the eastern South Atlantic Ocean: Evidence from benthic foraminifera, Palaeogeogr. Palaeocl., 130, 43–80, 1997.

Schmiedl, G., De Bovée, F., Buscail, R., Charriere, B., Hemleben, C., Medernach, L., and Picon, P.: Trophic control of benthic foraminiferal abundance and microhabitat in the bathyal Gulf of Lions, western Mediterranean Sea, Mar. Micropaleontol., 40, 167–188, 2000.

Schmiedl, G., Mitschele, A., Beck, A., Emeis, K-C., Hemleben, C., Schulz, H., Sperling, M., and Weldeab, S.: Benthic foraminiferal record of ecosystem variability in the eastern Mediterranean Sea during times of sapropel S_5 and S_6 deposition, Palaeogeogr. Palaeocl., 190, 139–164, 2003.

Schmiedl, G., Kuhnt, T., Ehrmann, W., Emeis, K.-C., Hamann, Y., Kotthoff, U., Dulski, P., and Pross, J.: Climatic forcing of eastern Mediterranean deep-water formation and benthic ecosystems during the past 22 000 years, Quaternary Sci. Rev., 29, 3006–3020, 2010.

Scholz, J. and Hillmer, G.: Reef-Bryozoans and Bryozoan-Microreefs: Control Factor Evidence from the Philippines and other Regions, Facies, 32, 109–144, 1995.

Siani, G., Paterne, M., Arnold, M., Bard, E., Métivier, B., Tisnérat-Laborde, N., and Bassinot, F.: Radiocarbon reservoir ages in the Mediterranean Sea and Black Sea, Radiocarbon, 42, 271–280, 2000.

Sierro, F. J., Hodell, D. A., Curtis, J. H., Flores, J. A., Reguera, I., Colmenero-Hidalgo, E., Bárcena, M. A., Grimalt, J. O., Cacho, I., Frigola, J., and Canals, M.: Impact of iceberg melting on Mediterranean thermohaline circulation during Heinrich events, Paleoceanography, 20, PA2019, https://doi.org/10.1029/2004PA001051, 2005.

Snousi, M.: Review of Certain Basic Elements for the Assessment of Environmental Flows in the Lower Moulouya, IUCN International Union for Conservation of Nature, Gland, Switzerland, 2004, https://groups.nceas.ucsb.edu/flow-experiments/documents/africa-sites/Review_of_certain_basic_elements_for_the_assessment_of_environmental_flows_in_the_Lower_Moulouya.pdf/at_download/filehttps://groups.nceas.ucsb.edu/flow-experiments/documents/africa-sites/ (last access: 17 August 2022), 2012.

Sparnocchia, S., Picco, P., Manzella, G., Ribotti, A., Copello, S., and Brasey, P.: Intermediate water formation in the Ligurian Sea, Oceanol. Acta, 18, 151–162, 1995.

Spezzaferri, S., Rüggeberg, A., Stalder, C., and Margreth, S.: Benthic foraminiferal assemblages from cold-water coral ecosystems, in: Atlas of Benthic Foraminifera From Cold-Water Coral Reefs, edited by: Spezzaferri, S., Rüggeberg, A., and Stalder, C.,

Special Publication/Cushman Foundation For Foraminiferal Research, 20–48, Vol. 44, Cushman Foundation, ISBN electronic 9781970168396, 2014.

Spötl, C. and Vennemann T. W.: Continuous-flow IRMS analysis of carbonate minerals, Rapid Commun. Mass. Sp., 17, 1004–1006, 2003.

Stalder, C., El Kateb, A., Vertino, A., Rüggeberg, A., Camozzi, O., Pirkenseer, C. M., Spangenberg, J. E., Hajdas, I., Van Rooij, D., and Spezzaferri, S.: Large-scale paleoceanographic variations in the western Mediterranean Sea during the last 34,000 years: From enhanced cold-water coral growth to declining mounds, Mar. Micropaleontol., 143, 46–62, 2018.

Stalder, C., Vertino, A., Rosso, A., Ruggeberg, A., Pirkenseer, C., Spangenberg, J. E., Spezzaferri, S., Camozzi, O., Rappo, S., and Hajdas, I.: Microfossils, a Key to Unravel Cold-Water Carbonate Mound Evolution through Time: Evidence from the Eastern Alboran Sea, PLoS One, 10, e0140223, https://doi.org/10.1371/journal.pone.0140223, 2015.

Suhr, S. B., Pond, D. W., Gooday, A. J., and Smith, C. R.: Selective feeding by benthic foraminifera on phytodetritus on the western Antarctic Peninsula shelf: Evidence from fatty acid biomarker analysis, Mar. Ecol. Prog. Ser., 262, 153–162, 2003.

Sun, X., Corliss, B. H., Brown, C. W., and Showers, W. J.: The effect of primary productivity and seasonality on the distribution of deep-sea benthic foraminifera in the North Atlantic, Deep-Sea Res. Pt. I, 53, 28–47, 2006.

Synal, H. A., Stocker, M., and Suter, M.: MICADAS: A new compact radiocarbon AMS system, Nucl. Instrum. Meth. B, 259, 7–13, 2007.

Taviani, M., Angeletti, L., Foglini, F., Corselli, C., Nasto, I., Pons-Branchu, E., Montagna, P.: U / Th dating records of cold-water coral colonization in submarine canyons and adjacent sectors of the southern Adriatic Sea since the Last Glacial Maximum, Prog. Oceanogr, 175, 300–308, 2019.

Tekken, V. and Kropp, J. P.: Climate-driven or human-induced; indicating severe water scarcity in the Moulouya River basin (Morocco), Water, 4, 959–982, 2012.

Terhzaz, L., Hamoumi, N., Spezzaferri, S., El Mostapha L., and Henriet, J. P.: Carbonate mounds of the Moroccan Mediterranean margin: Facies and environmental controls, C. R. Geosci., 350, 212–221, 2018.

Titschack, J., Thierens, M., Dorschel, B., Schulbert, C., Freiwald, A., Kano, A., Takashima, C., Kawagoe, N., Li, X., and IODP Expedition 307 scientific party: Carbonate budget of a cold-water coral mound (Challenger Mound, IODP Exp. 307), Mar. Geol., 259, 36–46, 2009.

Toucanne, S., Jouet, G., Ducassou, E., Bassetti, M.-A., Dennielou, B., Angue Minto'o, C. M., Lahmi, M., Touyet, N., Charlier, K., Lericolais, G., and Mulder, T.: A 130,000-year record of Levantine Intermediate Water flow variability in the Corsica Trough, western Mediterranean Sea, Quaternary Sci. Rev., 33, 55–73, 2012.

Tuenter, E., Weber, S. L., Hilgen, F. J., and Lourens, L. J.: The response of the African summer monsoon to remote and local forcing due to precession and obliquity, Glob. Planet. Change, 36, 219–235, 2003.

Van Krevelen, D. W.: Coal: typology–physics–chemistry–constitution, 3rd Edn., Elsevier Science Publishers, ISBN 9780444895868, 1993.

Van Rooij, D., Hebbeln, D., Comas, M., Vandorpe, T., Delivet, S., Nave, S., Michel, E., Lebreiro, S., Terrinha, P., Roque, C., Anton, L., Batista, L., and the MD194 Shipboard Scientists: MD 194/EUROFLEETS à bord du R/V Marion Dufresne. Cadix 10 Juin 2013 – Lisbonne 20 juin 2013, Les Rapports de Campagnes à la Mer, ISBN 2-910-180-81-6, https://archimer.ifremer.fr/doc/00416/52794/ (last access: 17 August 2022), 2017.

Viúdez, Á. and Tintoré, J.: Time and space variability in the Eastern Alboran Sea from March to May 1990, J. Geophys. Res., 100, 8571–8586, https://doi.org/10.1029/94JC03129, 1995.

Wang, H., Lo Iacono, C., Wienberg, C., Titschack, J., and Hebbeln, D.: Cold-water coral mounds in the southern Alboran Sea (western Mediterranean Sea): Internal waves as an important driver for mound formation since the last deglaciation, Mar. Geol., 412, 1–18, 2019.

Wang, H., Titschack, J., Wienberg, C., Korpanty, C., and Hebbeln, D.: The importance of ecological accommodation space and sediment supply for cold-water coral mound formation, a case study from the Western Mediterranean Sea, Front. Mar. Sci., 8, 760909, https://doi.org/10.1016/j.margeo.2019.02.007, 2021.

Wefing, A.-M., Arps, J., Blaser, P., Wienberg, C., Hebbeln, D., and Frank, N.: High precision U-series dating of scleractinian cold-water corals using an automated chromatographic U and Th extraction, Chem. Geol., 475, 140–148, 2017.

White, M.: Benthic dynamics at the carbonate mound regions of the Porcupine Sea Bight continental margin, Int. J. Earth Sci. 96, 1–9, 2007.

White, M., Mohn, C., De Stigter, H. C., and Mottram, G.: Deep-water coral development as a function of hydrodynamics and surface productivity around the submarine banks of the Rockall Trough, NE Atlantic, in: Cold-water Corals and Ecosystems, edited by: Freiwald, A. and Roberts, J. M., Springer-Verlag, Berlin, Heidelberg, 503–514, https://doi.org/10.1007/3-540-27673-4_25, 2005.

Wickham, H.: ggplot2: Elegant Graphics for Data Analysis, Springer-Verlag, New York, ISBN 331924275X, 9783319242750, 2016.

Wienberg, C.: A deglacial cold-water coral boom in the Alboran Sea: From coral mounds and species dominance, in: Mediterranean cold-water corals: past, present and future, edited by: Orejas, C. and Jiménez, C., Springer, 57–60, https://doi.org/10.1007/978-3-319-91608-8_7, 2019.

Wienberg, C. and Titschak, J.: Framework-forming scleractinian cold-water corals through space and time: a Late Quaternary North Atlantic perspective, in: Marine Animal Forests, edited by: Rossi, S., Springer, Switzerland, https://doi.org/10.1007/978-3-319-17001-5_16-1, 2016.

Wienberg, C., Hebbeln, D., Fink, H. G., Mienis, F., Dorschel, B., Vertino, A., Correa, M. L., and Freiwald, A.: Scleractinian cold-water corals in the Gulf of Cádiz – First clues about their spatial and temporal distribution, Deep-Sea Res. Pt. I, 56, 1873–1893, 2009.

Wienberg, C., Titschack, J., Freiwald, A., Frank, N., Lundälv, T., Taviani, M., Beuck, L., Schröder-Ritzrau, A., Krengel, T., and Hebbeln, D.: The giant Mauritanian cold-water coral mound province: Oxygen control on coral mound formation, Quaternary Sci. Rev., 185, 135–152, 2018.

Wienberg, C., Titschack, J., Frank, N., De Pol-Holz, R., Fietzke, J., Eisele, M. H., Kremer, A., and Hebbeln, D.: Deglacial

upslope shift of NE Atlantic intermediate waters controlled slope erosion and cold-water coral mound formation (Porcupine Seabight, Irish margin), Quaternary Sci. Rev., 237, 106310, https://doi.org/10.1016/j.quascirev.2020.106310, 2020.

Wilson, J. B.: "Patch" development of the deep-water coral *Lophelia Pertusa* (L.) on Rockall Bank, J. Mar. Biol. Assoc. UK, 59, Academic Press, https://doi.org/10.1016/B978-0-12-763150-9.50013-1, 1979.

Winston, J. E.: Feeding in marine bryozoans, in: Biology of Bryozoans, edited by: Woollacott, R. M. and Zimmer, R. L., 233–271, Academic, San Diego, California, Academic Press, https://doi.org/10.1016/B978-0-12-763150-9.50013-1, 1977.

Winston, J. E.: Feeding behaviour of modern bryozoans, in Lophophorates: Notes for a Short Course, Stud. Geol., Vol. 5, edited by: Broadhead, T. W., 1–21, Univ. of Tenn., Knoxville, Cambridge University Press, https://doi.org/10.1017/S0271164800000270, 1981.